copy #24

SRI

PROGRESS IN THE DEVELOPMENT OF A DIRECTION FINDING SYSTEM UTILIZING THE 8-LOOP FIXED SPACED LOOP ANTENNA

John D. Moore
W. M. Sherrill
Douglas N. Travers

INTERIM DEVELOPMENT REPORT FOR DIRECTION FINDER RADIO, SHIPBOARD SITING AND DESIGN, STUDY AND DEVELOPMENT

DDC

AUG 18 1972

C

Prepared for

NATIONAL TECHNICAL
INFORMATION SERVICE

SOUTHWEST RESEARCH INSTITUTE

SAN ANTONIO, TEXAS
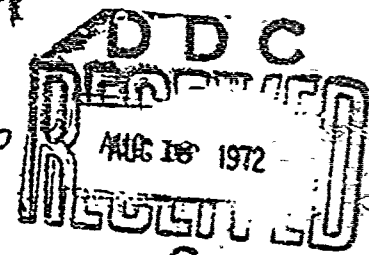
Best Available Copy

PROGRESS IN THE DEVELOPMENT OF A DIRECTION FINDING SYSTEM UTILIZING THE 8-LOOP FIXED SPACED LOOP ANTENNA

John D. Moore
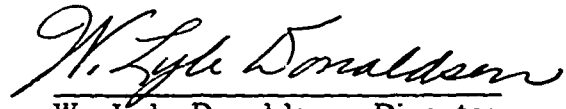W. M. Sherrill
Douglas N. Travers

INTERIM DEVELOPMENT REPORT FOR DIRECTION FINDER RADIO, SHIPBOARD SITING AND DESIGN, STUDY AND DEVELOPMENT

Period Covered: 1 May 1962 to 1 August 1962
Date of Report: 1 August 1962

Prepared for

APPROVED:

W. Lyle Donaldson, Director
Electronics and Electrical
Engineering

ABSTRACT

The development of a D/F system utilizing the 8-loop antenna (fixed spaced loop) is discussed. The feasibility of using this antenna with a goniometer or a twin channel technique has been previously reported. New results obtained with the 8-loop antenna and both the twin channel technique and the goniometer method are presented. An improved 8-loop goniometer system has been constructed to provide a laboratory breadboard to solve the basic engineering problems of the system.

The receiver requirements for a goniometer scan D/F system are discussed in detail with comparisons of the R-390A, RA.17C and the AN/SRD-7.

Other project work reported for the interim period includes phase stability measurements on the R-390A and RA.17C receivers. Detailed analysis of polarization response of spaced loop antennas is reported.

Brief discussions of the status of the hybrid transformer and the DFG-4 UHF direction finder are given.

TABLE OF CONTENTS

TABLE OF CONTENTS (Cont'd)

LIST OF ILLUSTRATIONS

LIST OF ILLUSTRATIONS (Cont'd)

PURPOSE

It is the purpose of this contract to derive engineering designs of practical shipboard radio direction finders, based on new concepts and techniques, which do not exhibit an appreciable reradiation error. Reradiation error results from the presence of secondary fields reradiated from the ship's superstructure. Recent progress in this field, resulting from previous contract NObsr-64585 with this laboratory, is to be continued and applied to new countermeasures systems for shipboard use. Othe new approaches to the reduction of reradiation errors, encountered for the first time only recently, are to be investigated.

Project Phase I: Study and evaluate present shipboard direction finder equipments and installations. Perform specific tasks as directed to etermine specialized performance of existing equipments in connection witn direction finder or countermeasures work.

Project Phase II: Formulate installation criteria which will assure greater uniformity of performance of installed equipment and, at the same time, simplify the task of installation. Perform specific tasks as required to determine the effect of site conditions on existing systems.

Project Phase III: Investigate the problems of equipment calibration with a view toward simplification of procedures and the utilization of automatic instrumentation to the greatest extent feasible.

Project Phase IV: Analyze and report the direction finding characteristics of antenna systems in shipboard environments. Emphasis is to be given to the development and application of direction finder analog techniques for investigating shipboard field configurations and investigating the effects of reradiation upon the response of typical antenna systems.

Project Phase V: Develop basic techniques and design criteria compatible with modern receiving systems which will enable the achievement of collector systems having greater immunity to the effects of the surrounding superstructure. Ferrite materials, component resolution direction finding, and the twin channel or multichannel receiver as a shipboard direction finding equipment are to receive special attention.

WORK PERFORMED

A. The 8-Loop D/F System

    1. Introduction and Review

        The spaced loop antenna when used in shipboard radio direction finding has been demonstrated under a previous contract (NObsr-64585) to have improved D/F performance in the presence of reradiation from the exis'ing superstructure of the ship.[1] As discussed in previous reports, the complexity of spinning loop systems at mast top installations makes it desirable to consider fixed passive antennas where the reliability can be significantly increased. Project effort has been directed toward the development of nonrc'ating spaced loop D/F systems for vertical polarizatior. which r^ssess increased reliability while retaining the advantages and bearing .' 'uracy o'>tained with the 3-loop (spaced loop) antenna. The feasibility of ,.ilizing a gon'ometer with crossed spaced loops or the 8-loop antenna, has been discussed in a previous report for this contract.[2]

        This 8-loop array is not to be confused with any 8-loop antenna so connected as to produce more than 4 nulls. The additional loops used over the usual number for a coaxial spaced loop only provide symmetry; they do not alter the mode of operation for vertical polarization.

        The feasibility of using the 8-loop antenna with a twin channel receiver was demonstrated and the initial test results were reported in the last interim report.[3] Work on the twin channel 8-loop D/F system was continued during the early part of the past interim period.

---

[1] "Shipboard Test of the Final Engineering Model of the Three-Loop Antenna on the U.S.S. Richard E. Kraus, " Interim Development Report, dated 26 August 1960, for Contract NObsr-64585.

[2] "Method of Goniometer Scanning the Coaxial Spaced Loop Direction Finder for Vertical Polarization, " Task Summary Report Number VIII, dated 1 April 1961, for Contract NObsr-85086.

[3] "Progress in the Development of a Twin Channel Spaced Loop Direction Finder, Interim Development Report, dated 1 May 1962, for Contract NObsr-85086.

2. The Twin Channel 8-Loop D/F System

a. Review

As reported in the previous interim report for this contract, the Racal RA. 153 twin channel receiver and MA. 190 indicator were received at this laboratory. Preliminary testing of the receiver and associated equipment was performed prior to the installation of the receiver for D/F purposes. Upon completion of these tests on the Racal RA. 153 twin channel receiver and MA. 190 indicator, the equipment was used with the 17-foot diameter 8-loop array for spaced loop twin channel direction finder tests. Successful operation of the system at 10 mc was reported, along with the calibration curve obtained at this frequency.[4] Evaluation of the twin channel 8-loop D/F system was continued (and is still underway) with primary emphasis placed on bearing accuracy tests within the frequency limit of the twin channel receiver. The concept of this antenna problem is now also to include through-mast installations (concentric mast through the center of the antenna).

b. Test Results

Bearing accuracy tests were made with the 17-foot diameter 8-loop antenna installed on the Southwest Research Institute 35-foot D/F tower. The twin channel equipment was installed in a screen room at the base of the tower in a manner similar to the preliminary breadboard arrangement described in the previous interim report.[5] Figure 1 is a block diagram of the test arrangement where the use of baluns rather than cathode followers for transformation from a balanced transmission line to the unbalanced input of the twin channel receiver is the only change from the same figure given in the previous interim report. Bearing accuracy tests were made at several frequencies between 3 and 29.5 mc.

Calibration curves for the bearing accuracy tests of the 8-loop twin channel system at 3 mc, 5 mc, 10 mc, 12 mc, 15 mc and 29.5 mc are given in Figure 2. The calibration curve at 3 mc shows an error spread of +2 and -3°, which is probably residual site error. No particular effort was made to reduce site error for these tests.

---

[4]"Progress in the Development of a Twin Channel Spaced Loop Direction Finder," Interim Development Report, dated 1 May 1962 for Contract NObsr-85086.
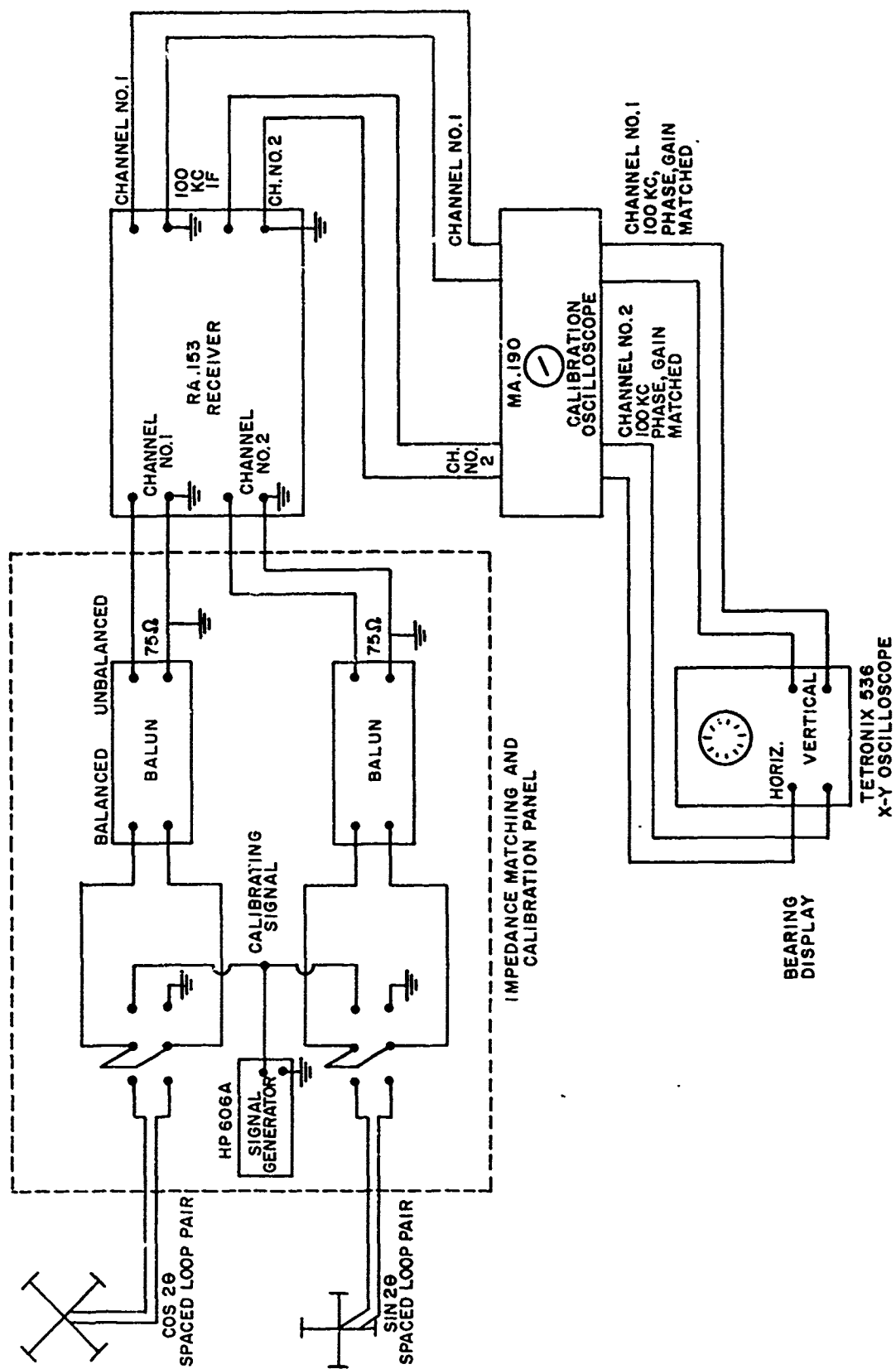
[5]Ibid.

FIGURE 1.

BLOCK DIAGRAM OF TWIN CHANNEL 8-LOOP DIRECTION FINDER.
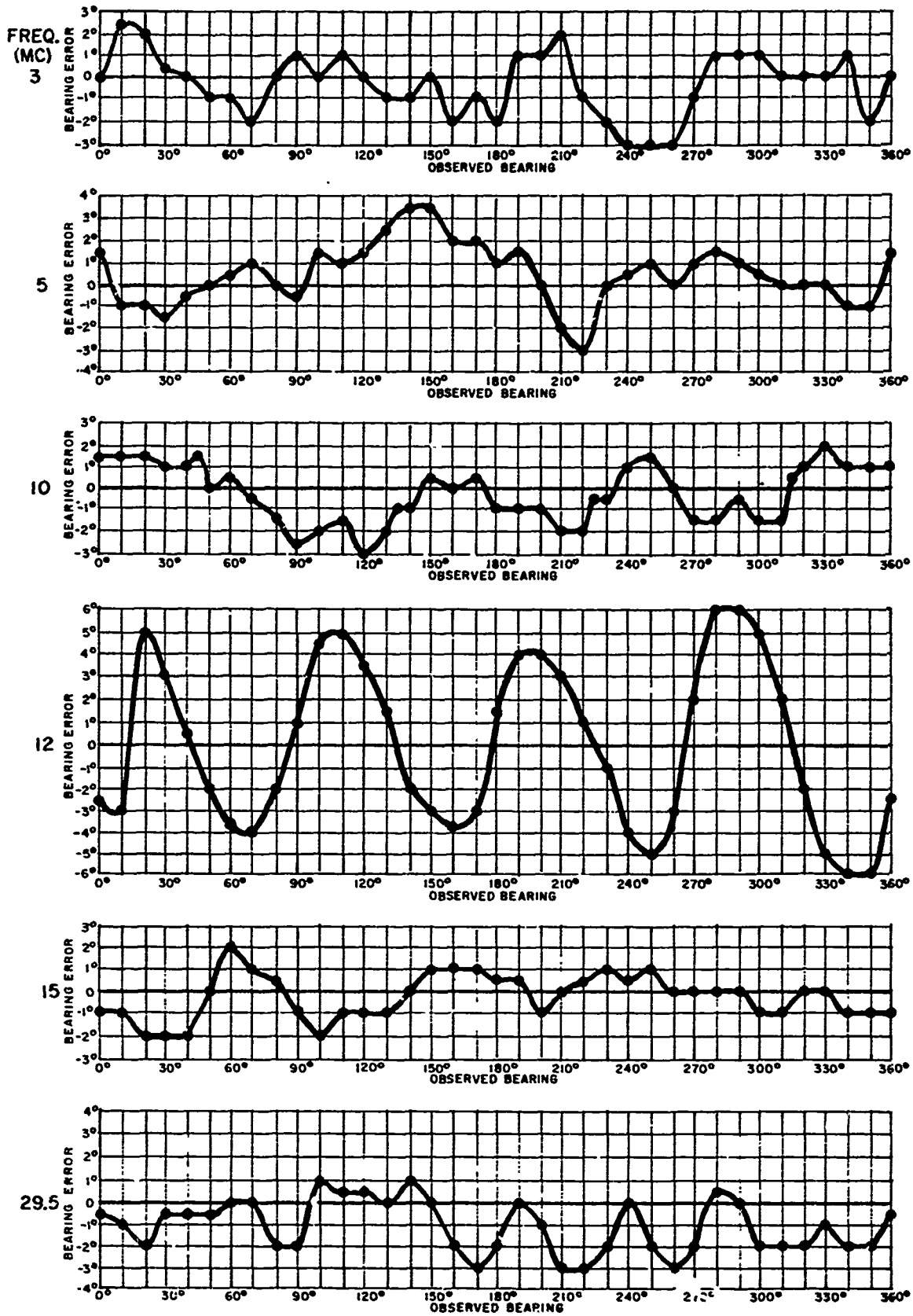
FIGURE 2.

CALIBRATION CURVES FOR THE 8-LOOP TWIN CHANNEL D/F SYSTEM.

It should be remembered, as discussed in the previous interim report, that the antenna pattern of the sin 2θ spaced loop group of four has considerable distortion at 3 mc caused by the resonant frequency of the Southwest Research Institute test mast. The source of the pattern distortion is thought to be the electrostatic field occurring at this resonance. The spaced loop pair located in the position of the cos 2θ spaced loop has good pattern quality at 3 mc. When the same antenna elements are relocated to the position of the sin 2θ spaced loop pair (physically rotated 45° at the top of the mast), deteriorated pattern performance results. This indicates that it is probably the position of the antenna at the top of the mast rather than the characteristic of the individual antenna which causes the difficulty.

Efforts have not been completed to reduce this electrostatic effect. It is believed that this condition is related to the manner in which the antennas are connected to the central hub or crossover box and from the fact that the box is bolted together rather than welded or soldered. It is known from past experience that spaced loop antennas are extremely sensitive to grounding asymmetry at the top of a mast, particularly at mast resonance.[6]

The 3-mc calibration curve in Figure 2 is still reasonable by the standards of the original rotating 3-loop antenna. In fact, it is as good as the calibration curve at 5 mc where no known pattern distortions occurred. One of the reasons why the 8-loop antenna, with the twin channel technique or a goniometer scan system, gives a superior performance with poorer individual antenna patterns is that cos 2θ, sin 2θ, antenna pairs produce one-half the observed bearing error for a given quality of pattern as compared to conventional crossed loops.[7]

The other calibration curves given in Figure 2 show reasonable error for a clean site up to 30 mc, with the exception of the curve at 12 mc. Proper termination of the transmission lines from the antenna was necessary to obtain acceptable bearing error performance at certain frequencies. The baluns shown in Figure 1 were adequate for this purpose.

The 12-mc curve exhibits a typical 8-node error function which is common to amplitude comparison D/F system when the amplitude

---

[6]"Methods for the Reduction of Reradiation Error in Naval High Frequency Shipboard Direction Finding," Final Development Report, dated 1 January 1961, for Contract NObsr-64585.

[7]"Progress in the Development of a Twin Channel Spaced Loop Direction Finder," Interim Development Report, dated 1 May 1962, for Contract NObsr-85086.

of the individual antenna pairs is not equal. The approximate self-resonance of the individual sin 2θ and cos 2θ crossed spaced loop antennas in the 17-ft diameter 8-loop antenna is found to be near 12 mc. Despite the fact that the antennas are constructed by similar techniques, they resonate at slightly different frequencies producing varying individual amplitudes near the self-resonant frequencies.

An investigation of bearing accuracy at the frequencies near the antenna self-resonance was conducted. With a target transmitter at 22-1/2 degrees where the error should be near a maximum value for unequal antenna amplitudes, the bearing was observed while the frequency was varied from 11.4 to 13.8 mc in small increments. Figure 3 shows the resulting error for this condition. It can be seen that as the frequency was varied, the bearing error increased to a maximum of approximately +6-1/2 degrees then decreased rapidly to a maximum negative error of approximately -9 degrees.

To clarify the data further, the Racal RA.153 twin channel receiver was disconnected and the amplitudes of the individual antennas were measured with an AN/PRM-1 field intensity meter from 12 mc to approximately 14 mc. The observed bearing was calculated by taking the arc tangent of the amplitudes of the two measured signals. The curve in Figure 4 was plotted from the calculations. It can be seen that the error curve for the calculated bearing versus frequency data is very similar to that obtained with the twin channel receiver.

The effective height of the 8-loop antenna has been measured for the purposes of future equipment sensitivity determination. The effective height data can be used as an aid in determining the antenna self-resonance. The effective height of the individual spaced loops of the 8-loop antenna is given in Figure 5. The theoretical effective height without the loss of the impedance matching cathode followers located at the antennas is also plotted in Figure 5. It can be seen that the effective height curve indicates an antenna self-resonance for both the sin 2θ and the cos 2θ spaced loop antennas near 12 mc where the bearing error has its largest value. The effective height curves indicate that the losses of the cathode follower impedance matching networks in the antennas are excessive. Improved cathode followers and other impedance matching devices are being investigated.

The basic error of the 8-loop antenna at the antenna self-resonance has been studied further with the goniometer scan technique as discussed later in this report. This source of bearing error is expected to be identical for either the twin channel or goniometer technique.
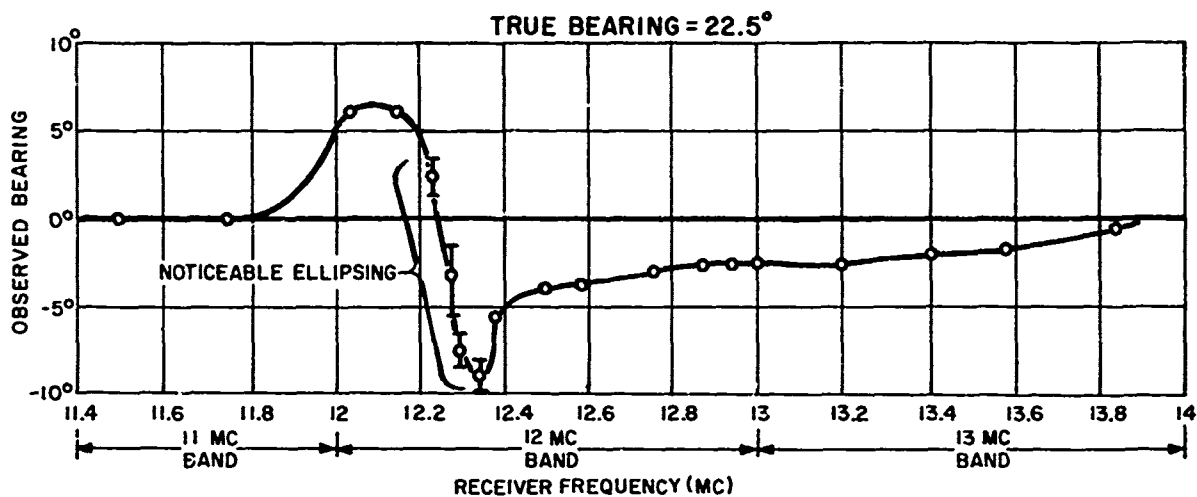
FIGURE 3.

BEARING ERROR VS. FREQUENCY FOR 8-LOOP TWIN CHANNEL SYSTEM,
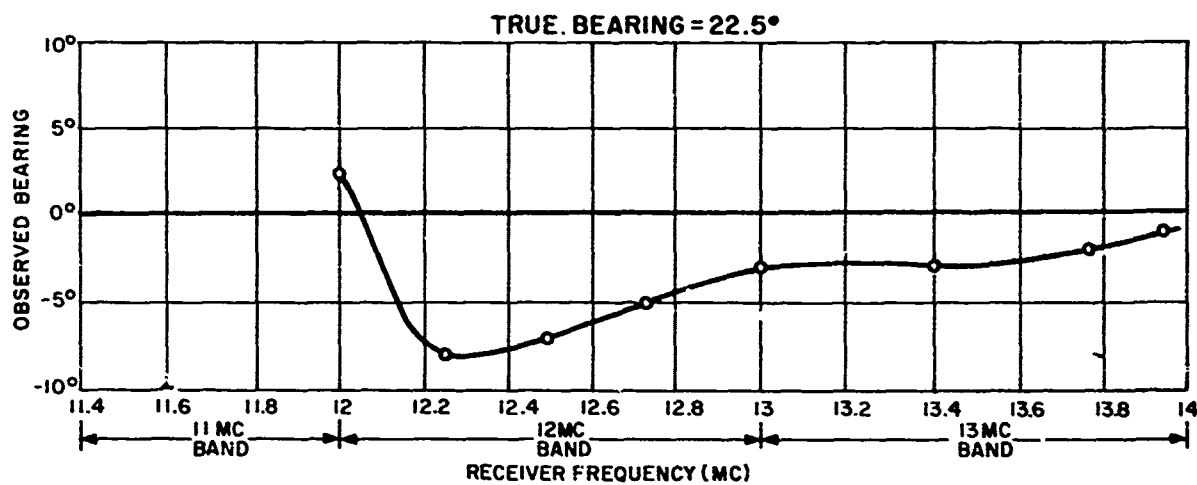NEAR ANTENNA SELF RESONANCE.

FIGURE 4.

BEARING ERROR VS. FREQUENCY FOR 8-LOOP TWIN CHANNEL SYSTEM, NEAR ANTENNA SELF
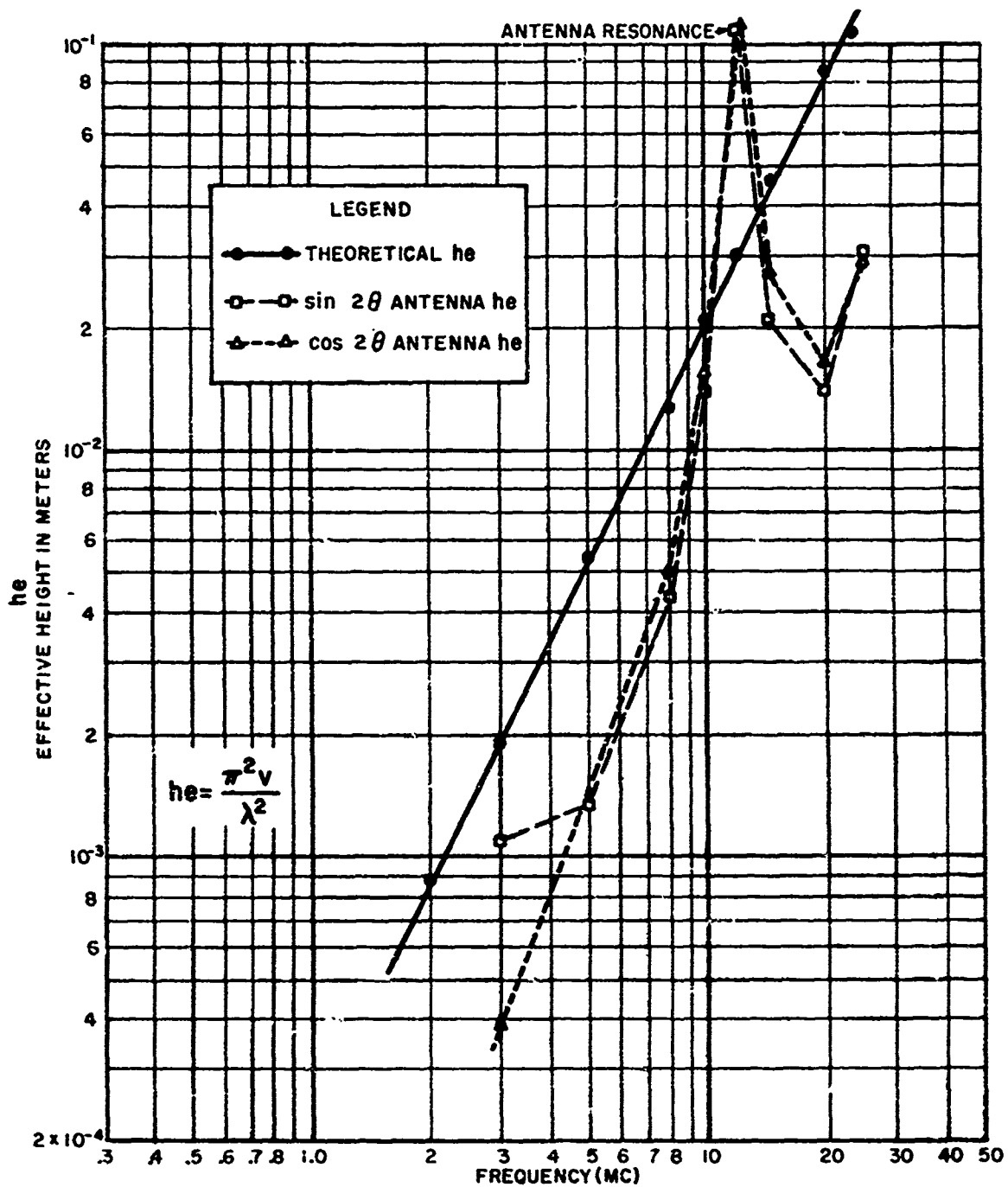RESONANCE. OBSERVED BEARING CALCULATED FROM MEASURED ANTENNA AMPLITUDES.

FIGURE 5.

EFFECTIVE HEIGHT OF THE INDIVIDUAL ANTENNAS OF THE 8-LOOP ANTENNA.

c.   Sense Tests with the Twin Channel 8-Loop D/F System

It is not practical to instrument instantaneous D/F and simultaneous sense with the Racal RA.153 twin channel receiver in its present configuration because a third channel is required. However, as explained in the previous interim report for this contract, the Racal RA.153 twin channel receiver and the MA.190 indicator have a feature whereby the individual loops of a crossed loop system may be sensed in turn against an omnidirectional antenna.[8] To sense the NS loop, the NS output is fed through one channel of the receiver to the vertical deflection plates of a CRT, while the sense signal is fed through the other channel of the receiver to the intensity grid of the CRT. The EW loop is sensed by feeding the output through the receiver to the horizontal plates of the CRT and the sense to the intensity grid of the CRT. This sense system requires a two-step switching operation because both of the crossed loop antennas must be compared on the cathode ray tube against the phase of the vertical sense antenna.

In the sense tests performed with the twin channel 8-loop D/F system, the cos 2θ spaced loop antenna was connected through channel 1 of the RA.153 twin channel receiver to the vertical deflection plates of the MA.190 indicator cathode ray tube. A vertical sense antenna, installed at the center of the 8-loop antenna, was connected to Channel 2 of the receiver with the IF output of this channel fed through the MA.190 indicator to the intensity grid of the cathode ray tube on the indicator. It should be remembered that voltage developed by a spaced loop antenna and the voltage developed by a vertical antenna are 180° out of phase if the antennas have the same phase center.[9] Consequently, a direct sense comparison may be made without the necessity of a phase shift network.

With the target transmitter at 0°, a sense indication in the form of a blanked trace at 180° was obtained which is correct in terms of the 180° phase difference between the two antennas. As the signal frequency was increased, it was found that a sense reversal was obtained, i.e., the position of the blanked trace moved from 180° to 0°, above the mast resonance of the Southwest Research Institute tower around 3 mc, as is to be expected with electrostatic sense antennas.

---

[8] "Progress in the Development of a Twin Channel Spaced Loop Direction Finder," Interim Development Report, dated 1 May 1962 for Contract NObsr-85086.

[9] "Methods for the Reduction of Reradiation Error in Naval High Frequency Shipboard Direction Finding," Final Development Report, dated 1 January 1961, for Contract NObsr-64585.

Experiments were also conducted using a shorted electrostatically shielded loop (one shorted turn) to determine if this antenna is suitable for sense at frequencies above the antenna mast resonance. Results were the same as those obtained with the vertical antenna described in the previous paragraph, in that sense reversals occurred at the same points.

d. Additional Twin Channel Equipment

A Racal RA. 117 receiver which is capable of being slaved to the RA. 153 twin channel receiver has been ordered. The RA. 117 slaved third channel receiver will provide the necessary channel for the sense signal to provide instantaneous D/F and sense for the twin channel system. The RA. 117 receiver is a modification of an existing production receiver and will require separate tuning of the first VFO and separate antenna tuning. Racal is working on a completely slaved third channel receiver as a companion to the production version of the RA. 153 twin channel receiver. The RA. 117 third channel will be adequate for evaluation work on the twin channel system deemed necessary by the Bureau of Ships and also will be a useful laboratory instrument in connection with the shipboard D/F program in general.

In addition to the RA. 117 third channel receiver, a Racal RA. 98A single sideband adapter has been received for use in conjunction with the Racal receivers.

The RA. 117 third channel receiver will be modified by Racal to provide for operation of the RA. 66B panoramic adapter which was received with the RA. 153 twin channel receiver. The RA. 98A single sideband adapter will be used with the RA. 117 third channel because the RA. 153 twin as it now exists is not compatible with this auxiliary equipment. Complete evaluation of the RA. 117 slaved third channel receiver, the RA. 66B panoramic adapter and the RA 98A single sideband adapter will be performed when the RA. 117 third channel receiver is received at Southwest Research Institute.

3. The 8-Loop Goniometer D/F System

a. Introduction and Review

The feasibility of scanning a crossed spaced loop with a goniometer has been discussed in a previous report for this contract.[10]

---

[10] "Method of Goniometer Scanning the Coaxial Spaced Loop Direction Finder for Vertical Polarization," Task Summary Report Number VIII, dated 1 April 1961, for Contract NObsr-85086.

Previous work demonstrated only the feasibility of the technique and left several basic engineering problems to be solved. For this reason, it was decided to build a new model which was sufficiently improved to provide a functional breadboard for the solution of the basic engineering problems known to exist for the goniometer scanned 8-loop antenna. It is now planned to extend this model to include through-mast installation of the antenna.

Basic problems in the development of the 8-loop goniometer system include errors caused by antenna self-resonance within the operating range, impedance matching between the reactive spaced loop antenna and the balanced transmission line, and proper impedance matching at the output of the goniometer. The goniometer output impedance match must be obtained for proper phase shift of one of the signals for adequate summing to provide the artificially developed 3-loop antenna pattern for simultaneous D/F and sense. For the current tests, an AN/SRD-7 receiver is being used, however the Racal equipment will also be used to study these basic problems.

b. The 8-Loop Goniometer D/F Breadboard

(1) Description of the Breadboard

A block diagram of the current 8-loop goniometer breadboard is given in Figure 6. The block diagram in Figure 6 contains planned sense components which were not installed at the time of the initial bearing accuracy tests. The two crossed spaced loops, which have output functions proportional to $\cos 2\theta$ and $\sin 2\theta$, respectively, are fed to impedance matching networks (accomplished by cathode followers at the present time) through matched lengths of RG-22/U balanced coaxial cable to the stators of the spaced loop goniometer.

The output of this goniometer is fed to the input of a standard AN/SRD-7 receiver. The detected video of the AN/SRD-7 receiver is fed to the AN/SRD-7 sweep system where it modulates a 40-kc subcarrier. This 40-kc subcarrier is fed to a sweep resolver which is driven in synchronization with the spaced loop goniometer but at one-half the speed of the goniometer. The output of the two stators of the resolver are fed to the vertical and horizontal deflection amplifiers in the AN/SRD-7 which drive the cathode ray tube to provide the D/F pattern.

Standard DAQ goniometers were used in the breadboard for both the simple loop and spaced loop. The DAQ goniometer has winding resonances in the vicinity of 22 mc which prevents its use above this frequency.
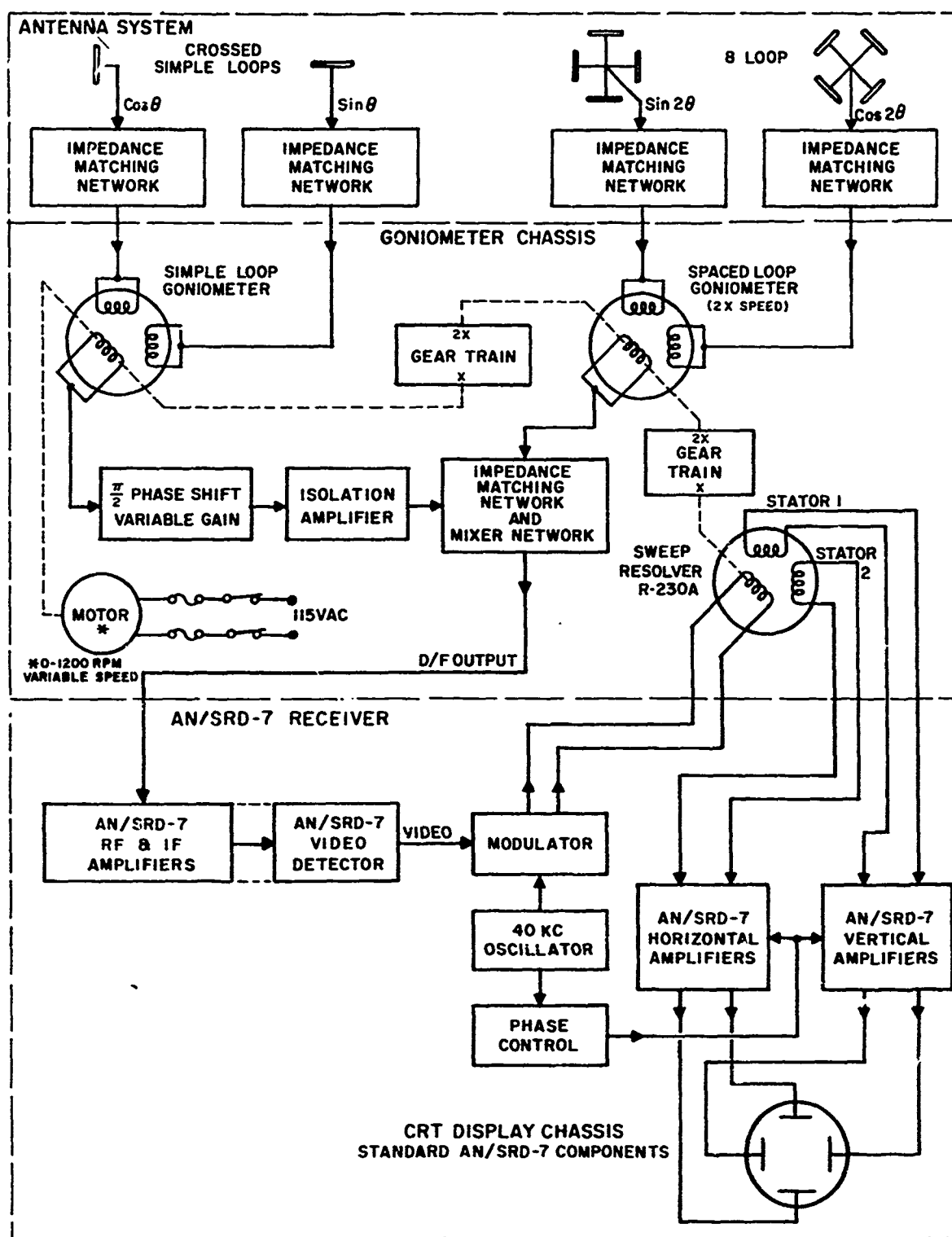
FIGURE 6.

8-LOOP GONIOMETER SYSTEM SIMPLIFIED BLOCK DIAGRAM.

A variable speed drive motor provides rotation rates between 0 and 1200 rpm for the simple loop goniometer. The simple loop goniometer is geared to the spaced loop goniometer with a step-up gear train to prcvide spaced loop goniometer rotation at twice the roiation speed of the simple loop goniometer. The spaced loop goniometer is geared to the sweep resolver through two to one gear reduction so that the sweep resolver rotates at the speed of the drive motor and simple loop goniometer.

The sweep resolver is located nearest the spaced loop goniometer because the greatest accuracy is desired from that goniometer. Adjusting the position of the sweep resolver housing with respect to the spaced loop goniometer provides a method for zeroing the D/F indication on the cathode ray tube. The spaced loop goniometer housing may be adjusted with respect to the simple loop goniometer to zero all three mechanical devices with the cathode ray tube display.

Plans have been made to replace the AN/SRD-7 receiver with a R-390A/URR receiver, the Racal RA.17C receiver, or any other suitable receiver suggested by the Bureau of ships. The Racal RA.153 twin channel receiver will also be used in tests with the goniometer system because the development of the twin channel technique will parallel the development of a goniometer scan system.

(2)   Bearing Accuracy Tests

Initial bearing accuracy tests were begun at approximately 12 mc where bearing error as a result of the individual antenna self-resonances had been observed with the twin channel system. The target transmitter was placed at an azimuth of 22-1/2°, and the bearing observed as the frequency of the transmitter was changed from 11.4 to 13.4 mc. The data of this are given in Figure 7. It can be seen that the bearing error versus frequency data for the goniometer scan system are almost identical to the data   tained with the twin channel receiver given in Figure 3. The pattern quality significantly deteriorated as the bearing error decreased from a positive to a negative value in Figure 7. Maximum blurring was estimated to be 70 percent.

Earlier workers often tuned crossed simple loops to the same frequency to increase sensitivity. This indicated that resonating the antennas to exactly the same frequency should improve the bearing error. A variable condenser with a 3- to 12- micromicrofarad range shunted by 1000 ohms was installed across the crossover connection of each spaced loop in the 8-loop antenna. With a signal near 12 mc, the spaced loop antenna believed to have the highest self-resonance frequency, the $\sin 2\theta$ spaced loop, was tuned to produce minimum blurring of the D/F pattern on the AN/SRD-7 CRT. Minimum blurring on the CRT would indicate that the phase of the two spaced loop signals feeding the goniometer were approximately the same or that they were resonant near the same frequency.
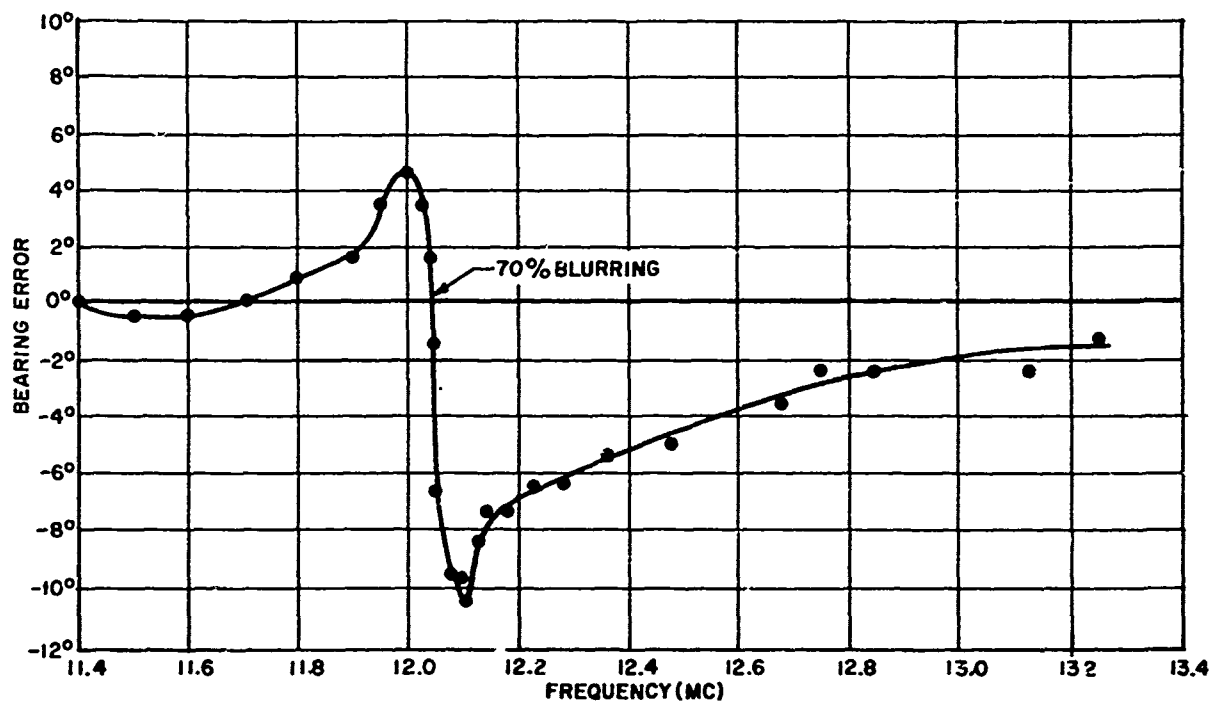
FIGURE 7.

BEARING ERROR VS. FREQUENCY AT ANTENNA RESONANCE WITH TARGET AT 22-1/2°-
INITIAL CONDITION.

FIGURE 8.
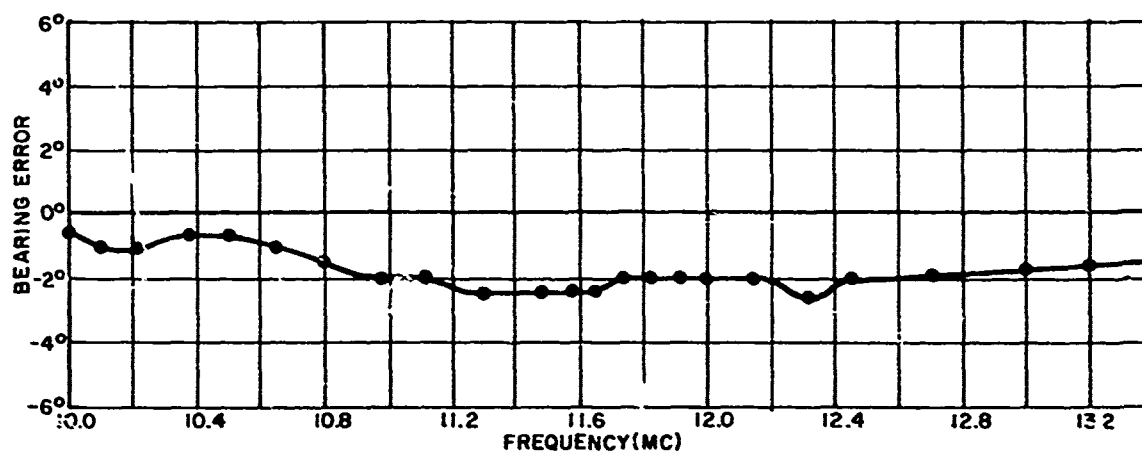
BEARING ERROR VS. FREQUENCY AT ANTENNA RESONANCE WITH TARGET AT 22-1/2°-
sin 2θ, ANTENNA TUNED FOR MINIMUM BLURRING.

A second bearing error versus frequency test was then completed from 10 mc to above 13.2 mc. The data are presented in Figure 8 where it can be seen that resonating the individual spaced loop antennas to the same frequency with a proper value of shunting resistor across each antenna results in a smooth bearing error curve over a wide frequency range. In addition, the severe blurring which had been obtained in the initial tests as shown in Figure 7 was not observed in tests of Figure 8.

A calibration curve had been obtained at the antenna self resonance of 12.1 mc for the initial condition. This calibration curve is compared in Figure 9 with a calibration curve at 11.65 mc, which was the new antenna self-resonant frequency, to show the change in bearing error for the two conditions. Partial curves completed at other frequencies between 11.65 and 12.1 mc indicated that the 11.65-mc curve was typical of the bearing error after the antennas were tuned to the same frequency and shunted by a 1000-ohm resistor.

With the solution for the antenna self-resonance bearing error effect, calibration curves were completed at several frequencies between 2 and 24 mc. The 24-mc frequency was dictated as an upper limit because of known self-resonance in the DAQ goniometers at approximately 22 mc. The calibration curves are given in Figures 10 and 11. The calibration curve at 2 mc in Figure 10 has excessive bearing error. The source of the error is believed to be the poor individual antenna pattern quality at this frequency. The 3-mc curve with a +2 and a -3-1/2° spread is similar to the 3-mc curve obtained with the twin channel system and the 8-loop antenna given in Figure 2. Calibration curves at 5 mc, 8 mc, 10 mc, 12 mc, 15 mc are reasonable curves for the Southwest Research Institute D/F site. The calibration curve at 18 mc exhibits slightly more error than curves at the lower frequencies, and, as the frequency is increased, the bearing error also increases. The source of the larger bearing errors at 2. mc are not known. However, the curve at 24 mc is probably affected by the self-resonance of the DAQ goniometer.

(3)   Sense Techniques

The most desirable sense indication for the 8-loop goniometer system is the 3-loop pattern which yields simultaneous D/F and sense. To artificially develop the 3-loop pattern in this system, a crossed simple loop antenna was installed at the center of the 8-loop antenna on the Southwest Research Institute D/F tower. This crossed simple loop antenna had loops which are approximately one foot square. The loops were fed to cathode followers for impedance matching through RG-22/U balanced coaxial cable to the simple loop goniometer as illustrated in Figure 6.
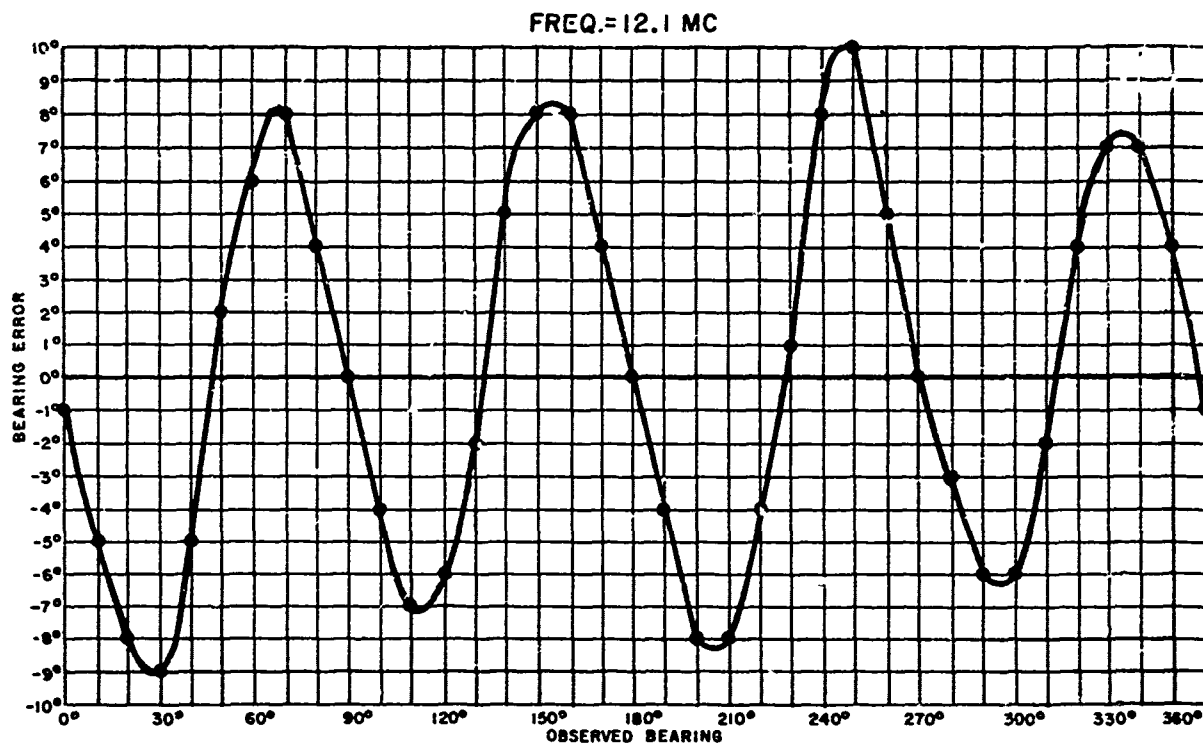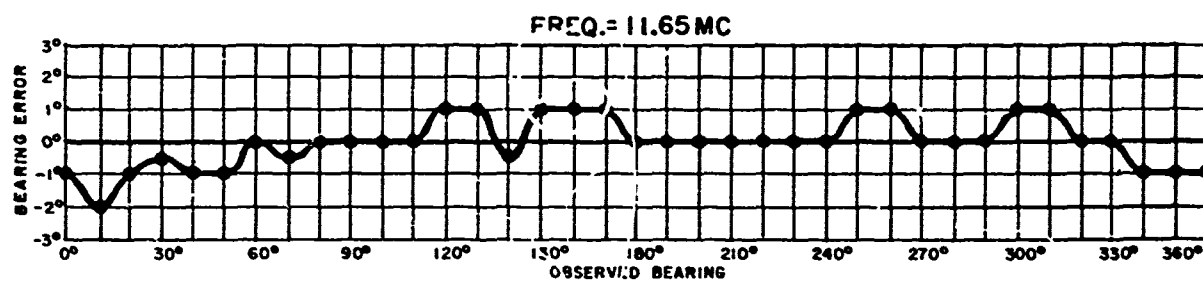
FIGURE 9.

CALIBRATION CURVES AT ANTENNA RESONANCE FOR 8-LOOP GONIOMETER SYSTEM,
BEFORE AND AFTER TUNING ANTENNAS TO SAME FREQUENCY.
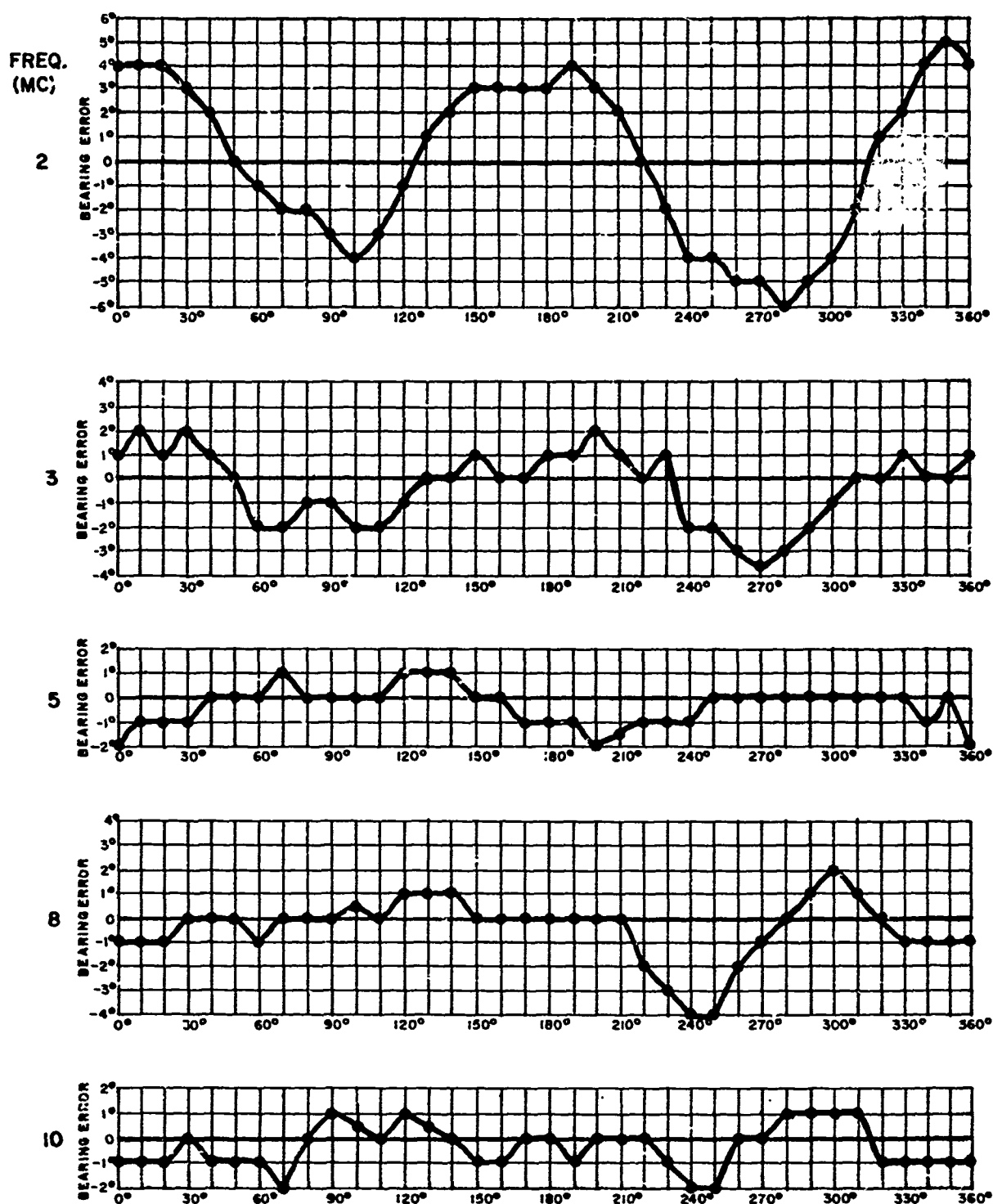
FIGURE 10.

CALIBRATION CURVES FOR THE BREADBOARD 8-LOOP GONIOMETER SYSTEM.
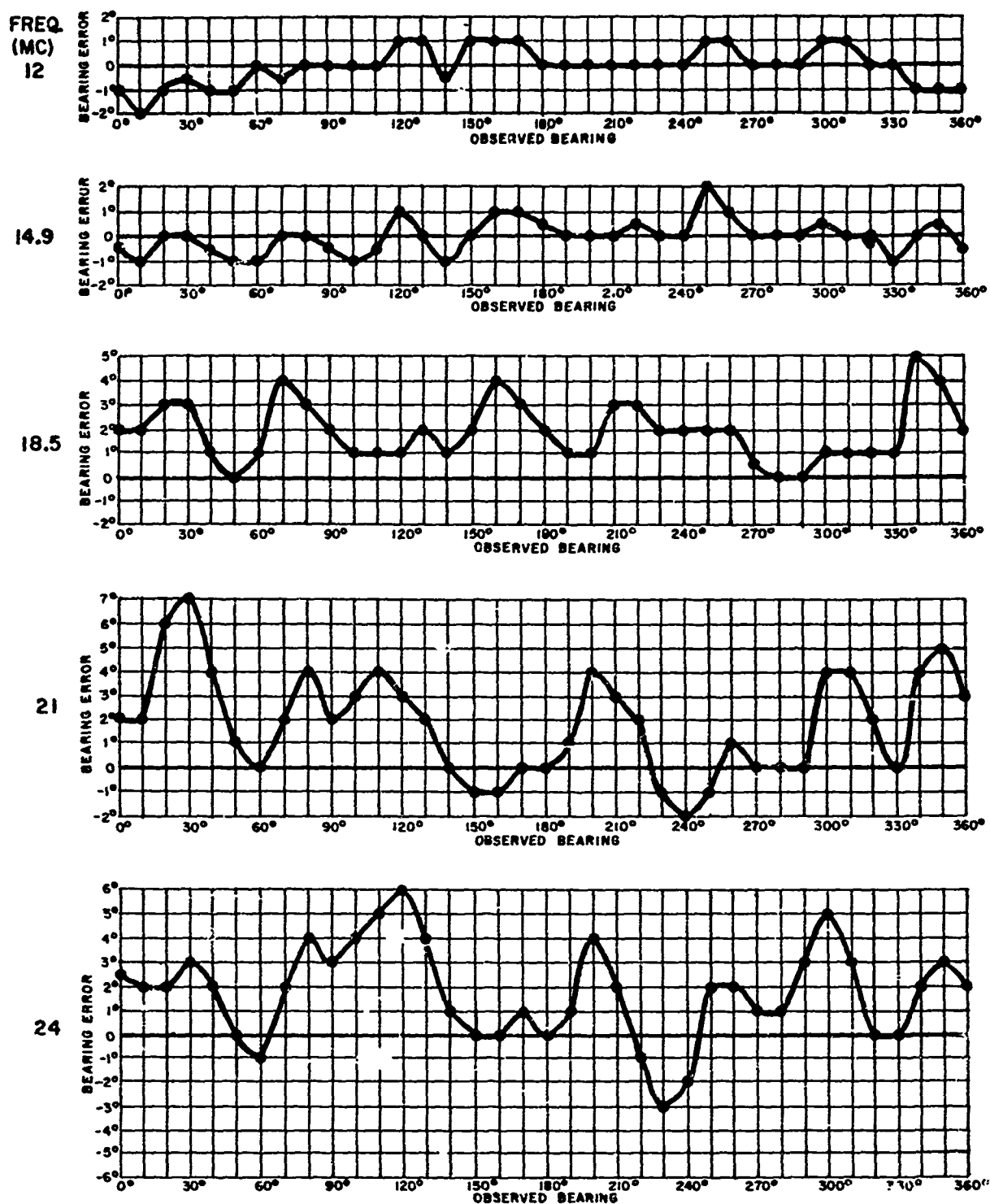
FIGURE 11.

CALIBRATION CURVES FOR THE BREADBOARD 8-LOOP GONIOMETER SYSTEM.

Successful 3-loop sense patterns were obtained between 2 and 7 mc with the test configuration as given in Figure 6. Patterns were obtained at 7 mc which indicated quadrature sense voltage. Above 7 mc, reversed sense occurred showing that a 180° phase reversal had occurred. Investigation of the goniometer circuitry revealed that a 7-mc resonance occurred in the output circuitry of the DAQ goniometer in the sense channel as a result of the reactance of the rotary transformer in the goniometer when 4-foot lengths of RG-22/U coaxial cable were connected to the goniometer and the phase shift circuitry. At the time of this writing, efforts are being made to match the goniometer output to the transmission line and phase shift circuitry to avoid the resonance and resulting sense reversals from this source.

Elimination of the sense reversal in the goniometer circuitry will enable the sense performance of the antenna system to be investigated. With the known self-resonance of the individual spaced loop antennas at 11.65 mc, sense reversals are anticipated above this frequency. If this occurs, all four antennas, the two spaced loops and the two simple loops, will be tuned to the same frequency and shunted with resistance to maintain equivalent phase relationships between the crossed spaced loop and crossed simple loop antennas. This technique has proven successful in screen room tests on rotating 3-loop antennas under another contract.

(4)   Bearing Sensitivity

The bearing sensitivity for ±5 degrees resolution of the 8-loop goniometer breadboard system was determined at 2, 4 and 8 mc before and after the antennas were tuned to the same frequency for antenna resonance bearing error effects. Initial data are given below.

Frequency, mc	Sensitivity for ±5° Resolution
2	1075 μv/m
4	425 μv/m
8	62.5 μv/m

A recheck of the bearing sensitivity after the antennas were tuned and shunted with resistance revealed approximately the same bearing sensitivity for ±5 degrees resolution.

This bearing sensitivity information does not reflect the optimum bearing sensitivity for the system. The antenna

cathode followers used in impedance matching between spaced loop antennas and transmission lines have a 6 to 8 db loss. Work is being conducted at the present time to develop an improved impedance matching technique for this application. Improved cathode followers, emitter followers and passive impedance matching techniques are being considered. Variable tuning of the antenna could produce considerable sensitivity increase.

c.   Servo Corporation of America Goniometers

A survey has been made to determine the availability of goniometers for the frequency range of 100 kc to 160 mc for use with the 8-loop goniometer system. The result of this survey revealed that Servo Corporation of America produces goniometers suitable for the frequency range of 100 kc to 30 mc in three units. The three units are the GO-9 which covers the frequency range of 100 kc to 1.5 mc, the GO-5A which covers the frequency range of 500 kc to 10 mc, and the GO-6A which covers the frequency range of 8 mc to 32 mc. One GO-9 goniometer, two GO-5A goniometers and two GO-6A goniometers were ordered.

At the time of this writing, the Servo goniometers models GO-9 and GO-6A have been received. The model GO-6A goniometer for the 8- to 30- mc range has been compared with a DAQ goniometer and will be incorporated into the 8-loop goniometer system at a later date. With the basic characteristics of the DAQ goniometer known, the DAQ goniometers will be used in the system while detailed impedance measurements are being made on the Servo GO-6A goniometers. Delivery of the GO-5A goniometer of Servo Corporation for the frequency range of 500 kc to 10 mc is not anticipated for a period of three to four months.

A literature search and study was begun along with limited experimentation for the purpose of constructing goniometers in the frequency range of 30 mc to 160 mc. Several approaches for the construction of goniometers are known, the best of which includes the ring goniometer which is not commercially available but is adequately described in the literature.[11]

d.   Comparative Receiver Performance for Goniometer D/F

Recent discussions with Bureau of Ships personnel have included the suggestion of using communications type receivers such as the R-390A or Racal RA.17C for D/F applications. Use of these single channel receivers in a D/F system requires a goniometer scan of the antenna output. The goniometer scan D/F places unique requirements on the receiver

---

[11]Ito, Yoji, and Tanaka, Isokazu, "Development of the Ring Goniometer for Radio Direction Finder, " IRE Transactions-Aeronautical and Navigational Electronics, December 1954, pp. 20-24.

and bearing indicator display circuits. The purpose of the tests described in the following paragraphs is to investigate the standard R-390A and RA.17C receivers as to suitability of bandwidth characteristics for D/F application.

(1)   D/F Receiver Bandwidth Requirements

The scanning of the antenna output by means of a goniometer results in amplitude modulation of the RF signal at the goniometer scan rate. The output of the goniometer is hence precisely similar to that of a carrier suppressed balanced modulator, possessing two sidebands separated from each other by twice the goniometer angular frequency (ω_m). An extensive analysis of the D/F receiver bandwidth requirements has been carried out by S. F. George.[12] The theoretical results given below follow his analysis of the bearing error and blurring effects introduced by receiver and bearing indicator circuitry.

The goniometer output and hence the receiver RF input signal is given by

$$E_{RF} = E_o \left\{ \sin \left[(\omega_{RF} + \omega_m)t + \delta + \phi_T \right] + \sin \left[(\omega_{RF} - \omega_m)t + \pi - \delta + \phi_T \right] \right\} (1)$$

where

ω_{RF} = the angular RF frequency

ω_m = the angular goniometer rotation frequency

δ = the true bearing of the incident plane waves

ϕ_T = an arbitrary phase constant

E_o = an amplitude factor

The above equation assumes ideal modulation by the goniometer with sidebands of equal relative amplitude and phase.

Passage of the modulated RF signal through the RF stages of the receiver may produce a change of amplitude and relative phase of the two sidebands. It is noted that the receiver is tuned to the nominal (suppressed) carrier frequency since $\omega_m << \omega_{RF}$. Because the two sideband frequencies may be unequally amplified through the RF stages,

---

[12]S. F. George, "Direction Finder Bandwidth Requirements," NRL Report No. R-3182, October 1947.

let the amplitude ratio of the two sidebands be γ_{SB} and the total phase shift of one sideband relative to the total phase shift of the other sideband be α_{SB}. Hence the output from the RF stages will be given by

$$E_{out(RF)} = AE_o \left\{ \gamma_{SB} \sin\left[(\omega_{RF} + \omega_m)t + \delta + \alpha_{SB} + \phi_{RF} \right] \right.$$
$$\left. + \sin\left[(\omega_{RF} - \omega_m)t + \pi - \delta + \phi_{RF} \right] \right\} \tag{2}$$

where

$$\phi_{RF} = \phi_T + \phi_r$$

ϕ_r = the phase shift obtained in the RF amplifier stages

A = RF amplification factor

The bearing information is obtained from the envelope of equation (2) and is given by

$$E_{oB}^2 = A^2 E_o^2 \left[1 + \gamma_{SB}^2 - 2\gamma_{SB} \cos 2\left(\omega_m t + \delta + \frac{\alpha_{SB}}{2} \right) \right] \tag{3}$$

Since the bearing is obtained at the zero (null) of equation (3), the observed bearing is obtained when equation (3) is set to zero, that is

$$\cos 2\left(\omega_m t + \delta + \frac{\alpha_{SB}}{2} \right) = \frac{1 + \gamma_{SB}^2}{2\gamma_{SB}}$$

For $\gamma_{SB} = 1$

$$2\left(\omega_m t + \delta + \frac{\alpha_{SB}}{2} \right) = \cos^{-1}(1)$$

however, for

$$0 \le \gamma_{SB} \le 1$$

$$\frac{1 + \gamma_{SB}^2}{2\gamma_{SB}} > 1$$

and hence no null occurs since $\cos \theta \not> 1$.

For the case of $\gamma_{SB} \neq 1$, the bearing is given by the minimum of equation (3), hence for the case

$$\gamma_{SB} \sin 2\left(\omega_m t + \delta + \frac{\alpha_{SB}}{2} \right) = 0 \tag{4}$$

if $\gamma_{SB} = 0$, the bearing is indeterminate, since one sideband amplitude equals zero. Hence the bearing is obtained for

$$\left(\theta + \delta + \frac{\alpha_{SB}}{2} \right) = 0, \ \pi, \ 2\pi, \ \ldots \ldots$$

or

$$\theta_{oB} = - \delta - \alpha_{SB}$$

(5)

where θ equals $\omega_m t$, the goniometer angle of rotation. Since the correct $\theta_{oB} = \delta$, the bearing error is given by

$$\epsilon = \frac{\alpha_{SB}}{2}$$

(6)

From the above analysis, it is seen that phase shift in the two sidebands produces bearing error without blurring (equation 6), while amplitude unbalance of the two sidebands produces blurring which may result in bearing error due to the broadness of the minimum. These results apply to the RF as well as to the IF sections of the receiver.

Bearing error and blurring may also occur because of harmonic distortion of the goniometer sidebands because of narrow IF bandpass characteristics or distorted output of the video detector (or "second detector") which feeds the CRT bearing indicator deflection circuits. This harmonic distortion requirement implies the necessity of sufficiently wide bandwidth for the IF and indicator circuits. Indicator circuitry bandwidth requirements are generally considered separately from the receiver proper and are associated with the problem of automatic bearing indication. Thus, the indicator problem will not be further discussed here.

(2)   Experimental Investigation of Receiver Bandwidth Effects

An experimental investigation of the performance of the R-390A and RA.17C communications receivers as regards bandwidth requirements for proper D/F performance has been carried out. The block diagram of Figure 12 shows the experimental arrangement used. Signals from the 17-foot diameter 8-loop array are fed through the spaced loop goniometer to the communications receiver in question. The goniometer is driven by a variable speed motor which enables data to be taken at different modulation frequencies. Both receivers were provided with an external IF output jack at the back panel of the receiver. This IF output signal is amplified, detected and fed to the deflection circuits of an AN/SRD-7 shipboard direction finder.
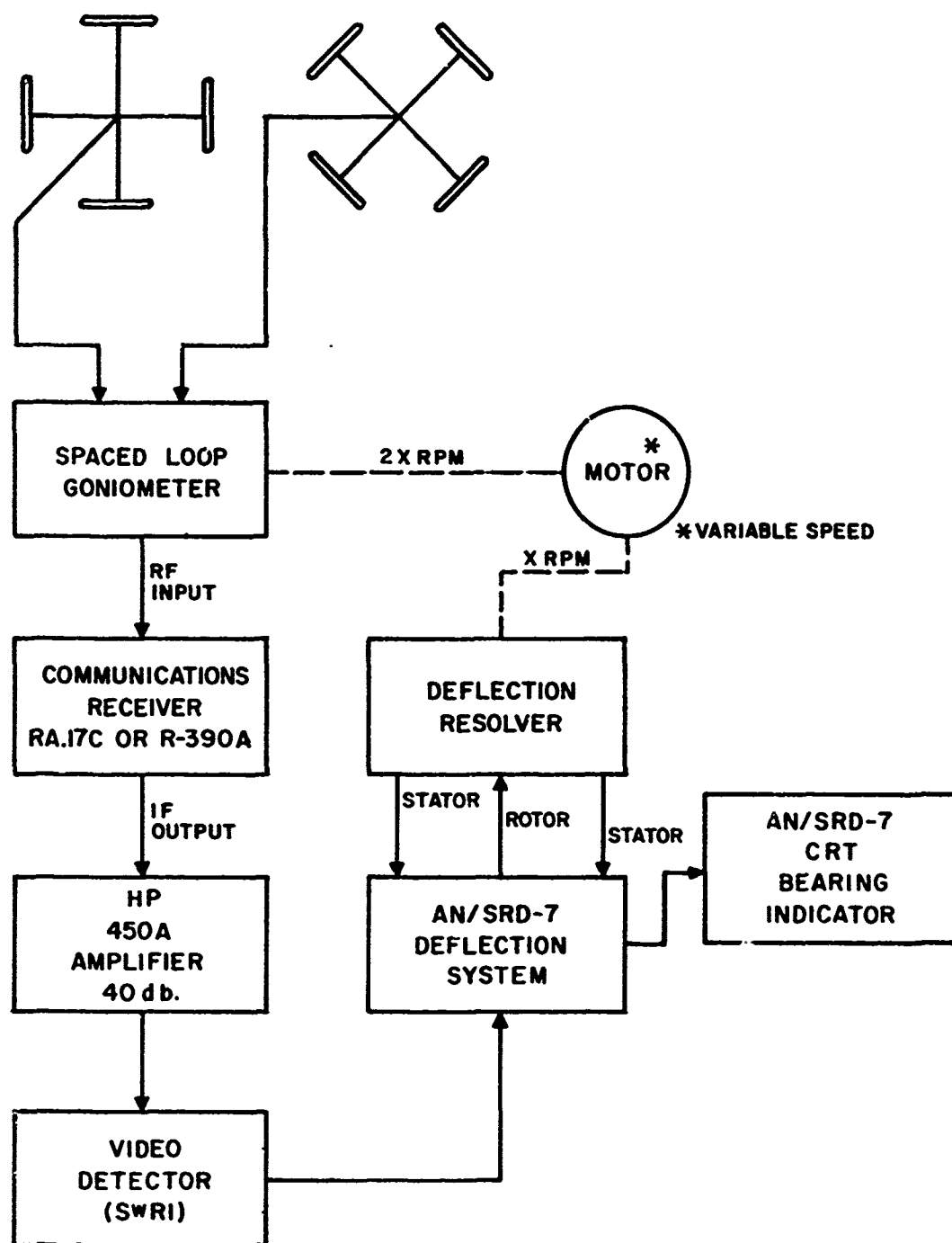
FIGURE 12.

BLOCK DIAGRAM OF GONIOMETER D/F SYSTEM FOR COMPARISON
OF RECEIVER PERFORMANCE.

The target vehicle was stationed at 0' azimuth on the Southwest Research Institute calibration track. The test frequency used was approximately 10 mc. Utilizing the wide tuning dial band spread of both the RA. 17C and R-390A, the observed bearing versus tuning frequency was observed for the various IF bandwidths available at the receiver. These data are obtained for both fast (40 rps) and a slower (4 rps) goniometer rotation speed and hence modulation frequency. In this way, the effects of receiver IF bandwidth and RF tuning could be observed as regards the constancy of observed bearing.

R-390A

The balanced output of the spaced loop goniometer was fed to the 125-ohm balanced input of the R-390A in order to obtain maximum sensitivity. The curves of Figure 13 show the observed bearing versus frequency obtained for each of the bandwidths available from the R-390A.

Two sets of data were obtained, one utilizing a four-cycle per second goniometer rotation rate, the other using a 40-cycle per second goniometer rotation rate. It is seen from the curves of Figure 13 that for the slow goniometer rotation, satisfactory observed bearings (bearing variation not greater than 10) were obtained as a function of tuning for the 16-kc, 8-kc and 4-kc bandwidths. For the fast goniometer scan rate, a constant observed bearing was obtained for the 16-kc bandwidth only while a 1-degree variation was observed at the 8-kc bandwidth. For bandwidths below 8 kc, observed bearings varying 6 degrees or more total were observed as a function of tuning. It is further noted that as the bandwidth is decreased from 4 kc to 0.1 kc, the variation in observed bearing increased so that, at the narrowest bandwidth, a variation of 23 degrees maximum for the fast goniometer scan rate is obtained.

Bearings observed at the slow rate are significantly different from bearings observed at the fast goniometer scan rate. This implies that for a given goniometer rotation rate, the goniometers should be zeroed to give an accurate observed bearing at 0 degrees. This adjustment of the goniometer will hold for a particular rotation rate only. It is also noted from these data that a narrower receiver bandwidth may be tolerated for reduced goniometer scan rate; however, the D/F response time of the system is reduced proportionately. For the case of the 40-cycle scan rate, a bandwidth less than 8 kc probably could not be tolerated utilizing a standard R-390A receiver.
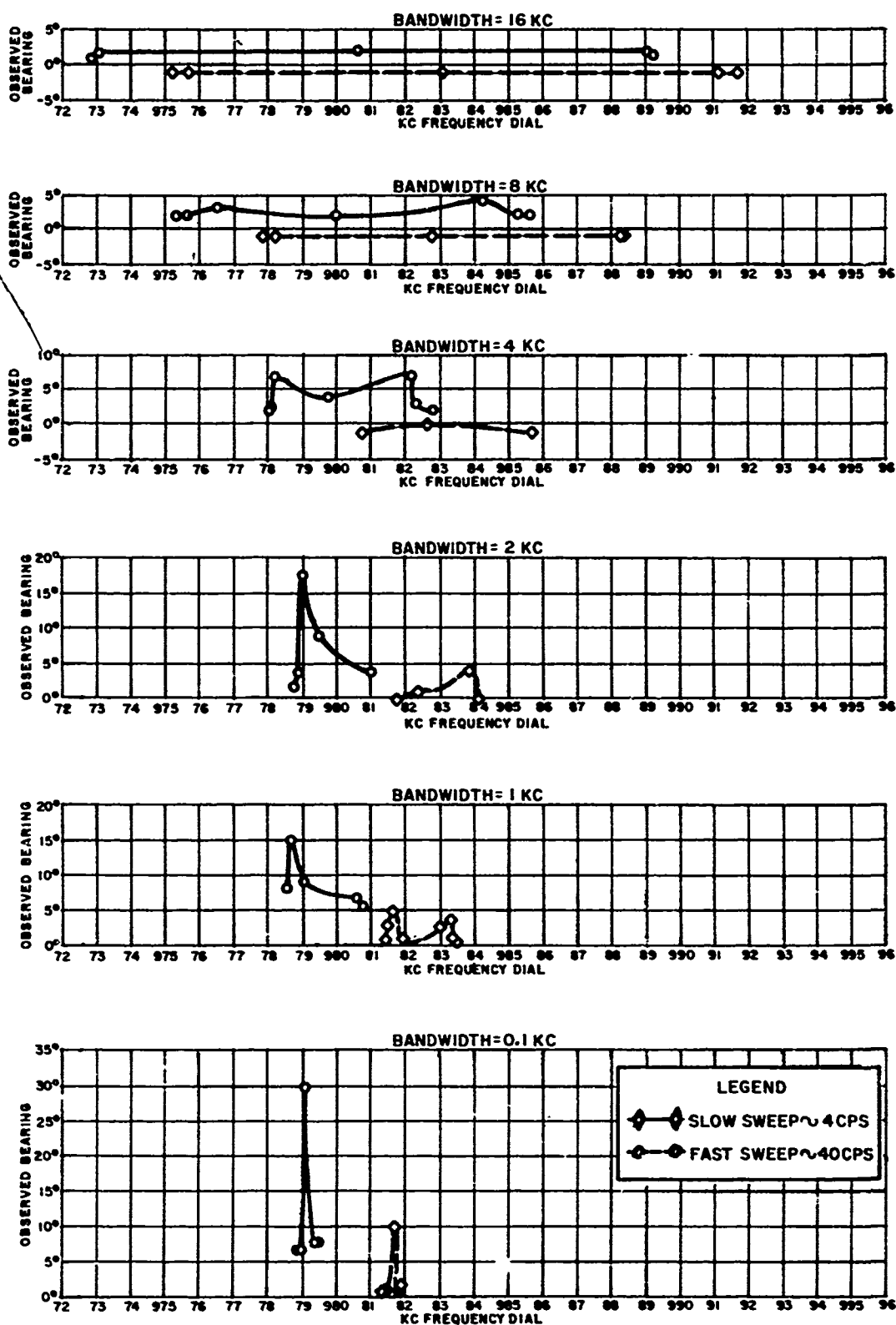
FIGURE 13.

R-390A OBSERVED BEARING VS. KC TUNING FOR VARIOUS BANDWIDTHS.

RA. 17C

Data were obtained on the Racal RA. 17C for
the tuned mode of operation. The balanced goniometer output was fed
through a 110-ohm balanced to 75-ohm unbalanced balun to the 75-ohm
unbalanced input of the RA. 17C. The goniometer scan rates of four
cycles and 40 cycles were used to obtain observed bearing versus kc
tuning frequency.

The data of Figure 14 show that a total shift
in observed bearing of no more than 1 degree may be obtained for the
13 kc and 6.5 kc bandwidths for the four-cycle goniometer scan rate.
For the 40-cycle scan rate, a 3-degree shift in bearing is observed at
the 6.5-kc bandwidth. Constant observed bearings were obtained at the
13-kc bandwidth only. At the 0.1-kc bandwidth as much as 43 degrees
of bearing shift were obtained at the 40-cycle scan rate, while at the four-
cycle scan rate 21 degrees of bearing shift were observed. It should be
noted that at both the 0.3-kc and 0.1-kc bandwidths the bearing indicator
pattern quality was extremely degraded including blurring and severe
pattern distortion.

The difference in observed bearing obtained
for the slow scan rate and the fast scan rate was found to hold true for
the RA. 17C receiver also. As with the R-390A, the shift of bearing as
a function of tuning was minimized as the goniometer scan rate was
reduced.

AN/SRD-7

Data were obtained on the observed bearing
versus tuning frequency for the AN/SRD-7 receiver. These data were
obtained for comparison with those given above for the R-390A and RA. 17C
communications receivers. The AN/SRD-7 receiver is comparable in
sensitivity to the RA. 17C. The observed bearing using the AN/SRD-7 was
found to be invariant as a function of tuning frequency and goniometer scan
rate.

Only one bandwidth is available in the SRD-7.
This is a 3-kc bandwidth at 6 db down provided by tuned IF amplifiers.
It is seen that the observed bearing variation for the AN/SRD-7 is as
constant at 3 kc as the same observed bearing variation for the two
communication receivers at maximum bandwidth. Furthermore, no
observed bearing variation was obtained for either the slow or the high
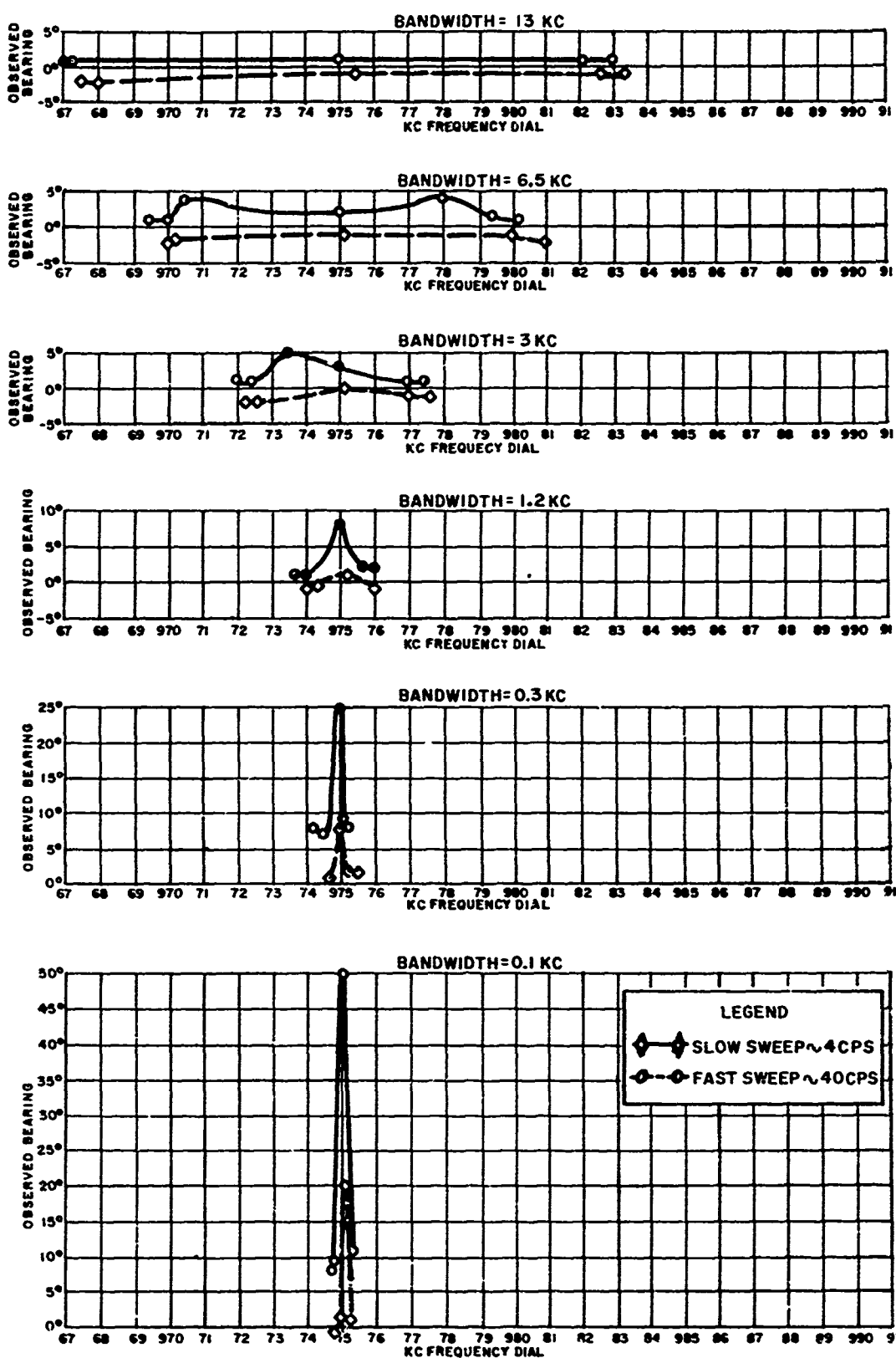speed goniometer rotation.

FIGURE 14.

RA.17C OBSERVED BEARING VS. KC TUNING FOR VARIOUS BANDWIDTHS.

It must be emphasized that in the tests described above the only system variable was the D/F receiver. For the case of the R-390A and RA.17C, IF bandwidth is determined by IF filters which may be selected from the front panel. For bandwidths greater than 2 kc in the R-390A, mechanical filters are provided, and for the 1- and .1-kc bandwidths a crystal filter in addition to a mechanical filter is provided. For the RA.17C, LC filters provide bandwidth selectivity from the 1.2 to 13 kc bandwidths. The 0.3 and 0.1 kc bandwidths are provided by crystal filters in addition to LC filters. A more complete description along with IF bandpass curves is provided in Task Summary Report XI for this contract where an extensive comparative evaluation of the two receivers was reported. [13]

Comparison of the IF circuitry of the two communication receivers and the AN/SRD-7 shows that extreme care was taken in the bandpass characteristics of the AN/SRD-7 so that no bearing error would occur as a function of tuning frequency. This implies that no differential phase shift occurs between the sidebands of the goniometer modulating signal in the IF sections. The extreme bearing variations observed in both the communications receivers for bandwidths less than 8 kc shows the IF filters apparently produce differential phase shift between the sidebands of the modulated goniometer signal. A consideration of Figures 13 and 14 shows that operation of the receivers in the widest bandwidth (16 kc for the RA-390A and 13 kc for the RA.17C) is required for constant observed bearing as a function of tuning frequency. Satisfactory D/F operation could be obtained, however, using the next narrower bandwidth, that is, 8 kc for the R-390A and 6.5 kc for the RA.17C.

Earlier work with filtering of the video output of an AN/SRD-7 receiver indicated definite video bandwidth requirements; however, the results were not as severe as those obtained with the R-390A and RA.17C receivers. [14] From the test data, it may be concluded that extreme care must be taken in the bandpass characteristics of the IF section of D/F receivers. Such linear gain and phase characteristics are not maintained by these communications receivers in the standard models for bandwidths less than 6 kc. Use of the R-390A and RA.17C as D/F

---

[13]"Comparative Evaluation of the Racal RA.17C-12 and Collins-Motorola R-390A/URR Receivers," Task Summary Report Number XI, dated 15 May 1962, for Contract NObsr-85086.

[14]"Assembly of the Three Loop Antenna and an Investigation of Improved Methods for Reducing Reradiation Error," Interim Development Report for Contract NObsr-64585, dated 26 July 1959.

receivers is optimum for the broadest bandwidth configurations. Operation of the receivers as D/F receivers in the 3- or 4-kc bandwidth positions would require significant modification.

B.   Phase Stability Comparison of the R-390A and RA. 17C Receivers

At the request of the Bureau of Ships, an investigation was carried out to observe the phase stability of the R-390A and the RA. 17C communications receivers. An extensive evaluation and comparison of these two receivers has been carried out in this laboratory and is reported in Task Summary Report XI.[15] A detailed description of the two receivers and a comparison of their sensitivity, bandwidth, and other characteristics is given in that report.

The investigation of the phase stability of the R-390A and RA.17C included a measurement of the phase shift from the RF input to the IF output of the receiver as a function of IF bandwidth. Phase stability for the purpose of this report implies a constant phase shift from the RF input to the IF output as a function of bandwidth without sudden anomalous changes of phase as a function of time. In the paragraphs to follow, the phase shift data will be presented for the selectable bandwidths of each receiver at the several frequencies. These frequencies show the phase stability at various settings of the megacycle VFO and kilocycle VFO.

The block diagram of the experimental arrangement for measuring phase stability is shown in Figure 15. The method of measuring front-to-back phase shift involved modulating an RF carrier at a low audio frequency. This signal was fed to the RF input of the receiver in question. The IF output of the receiver was fed to a demodulator and the demodulated audio frequency signal was then fed to the vertical deflection plates of a Tektronix Model 536 X-Y Oscilloscope. The horizontal deflection plates of the X-Y oscilloscope were fed by the audio modulating signal. In this way, phase shift could be measured from the front end of the receiver to the IF output with an ambiguity amounting to some integral number of 2π radians. The audio modulating frequency was chosen to be 30 cycles, a frequency which was low enough to produce sidebands that would be separated by a small fraction of a bandwidth for most of the bandwidths provided by the receivers. This frequency was also high enough to be passed by the demodulator provided without significant attenuation.

---

[15]"Comparative Evaluation of the Racal RA. 17C-12 and Collins-Motorola R-390A/URR Receivers, " Task Summary Report Number XI, dated 15 May 1962, for Contract NObsr-85086.
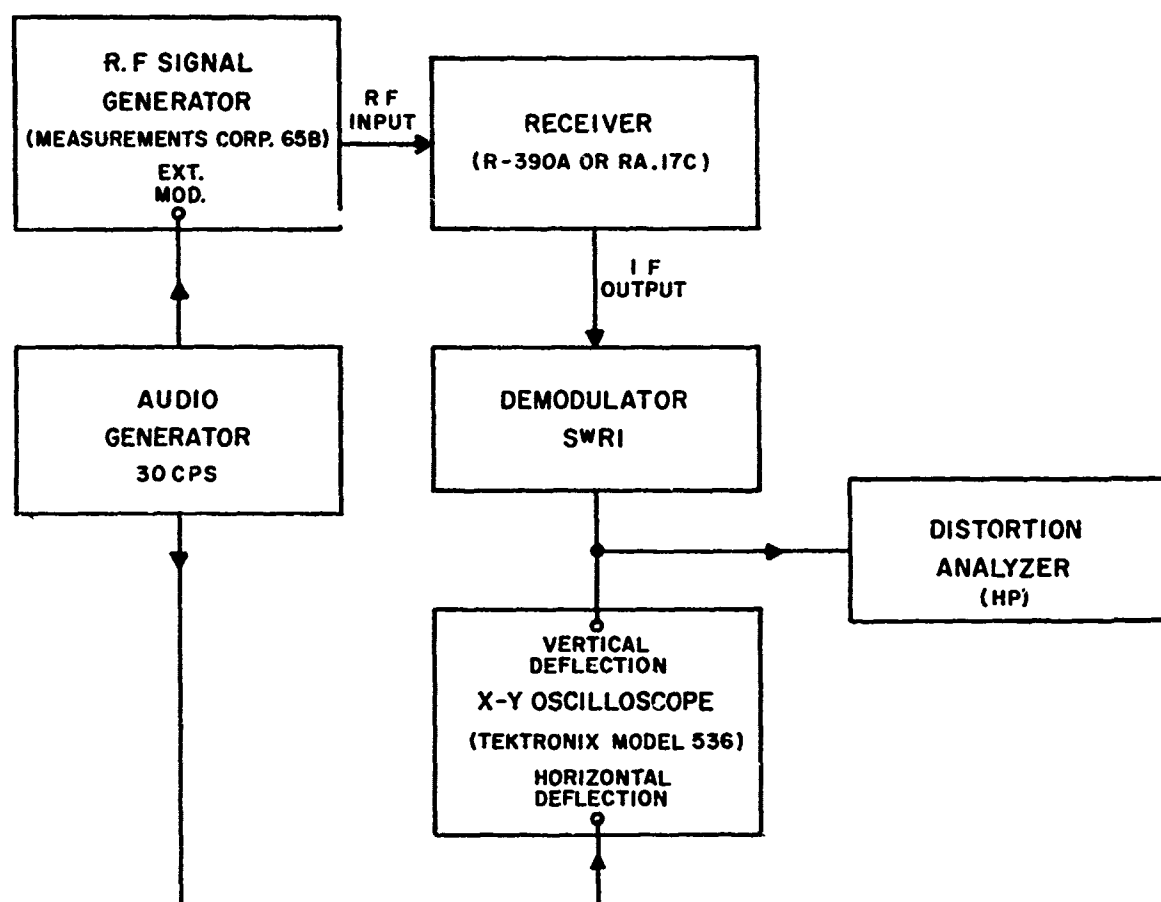
FIGURE 15.

TEST ARRANGEMENT FOR DISTORTION AND PHASE MEASUREMENTS
FOR RA.17C AND R-390A RECEIVERS.

The phase shift measuring method requires sine wave inputs to the X-Y oscilloscope at both channels. It was found that especially for the narrower bandwidths excessive distortion was obtained for the 30-cycle signal. Therefore, a distortion analyzer was used to get a quantitative measure of the distortion present in the receiver demodulated output.

A preliminary experiment was made to determine the harmonic distortion of the 30-cps signal in the audio generator, RF signal generator, and demodulator system. The externally modulated RF signal was demodulated and fed to the distortion analyzer with the result that no greater than 1 percent of distortion was observed in the system. Thus, any distortion read for the case of an extremely distorted phase measuring ellipse is primarily due to the receiver distortion. It was found that suitable phase measurement could be obtained for distortions under not greater than 30 percent, therefore, the 1 percent distortion of the audio generator, RF signal generator, and demodulator system is negligible.

1. R-390A Phase and Distortion Data

The histograms of Figure 16 show the phase shift measured from the receiver front end to the IF output and the percent harmonic distortion of the IF output as a function of bandwidth obtained for the R-390A receiver. Phase and distortion measurements were made at the frequencies 1.5, 5.5, 10, 10.5, 10.9, 15.5 and 23.5 mc. The receiver was tuned for maximum IF output for all phase and distortion measurements. It is seen that for all frequencies the front-to-back phase shift varies by less than 10 degrees for all bandwidths from the 0.1-kc to the 16-kc bandwidth. Percent distortion is seen to approach 30 percent for frequencies at 15.5 and 23.5 mc for the lowest bandwidths, that is, 0.1 kc and 1kc.

Phase measurements were possible for all bandwidths and frequencies below 24.0 mc, although some significant distortion and hence a somewhat distorted phase measuring ellipse was observed at the higher frequencies. The total variation of phase shift for all frequencies ranges from 75 degrees to 55 degrees, although at any frequency chosen the range of phase shift as a function of bandwidth does not exceed 10 degrees. The 23.5-mc upper frequency was chosen because at frequencies above 23.5 mc satisfactory phase shift measurements could not be made. This implies that distortion significantly greater than 20 percent was obtained at frequencies greater than 23.5 mc.

Throughout this set of observati·· , anomalous phase shift as a function of time was not observed. It is re-emphasized that in all
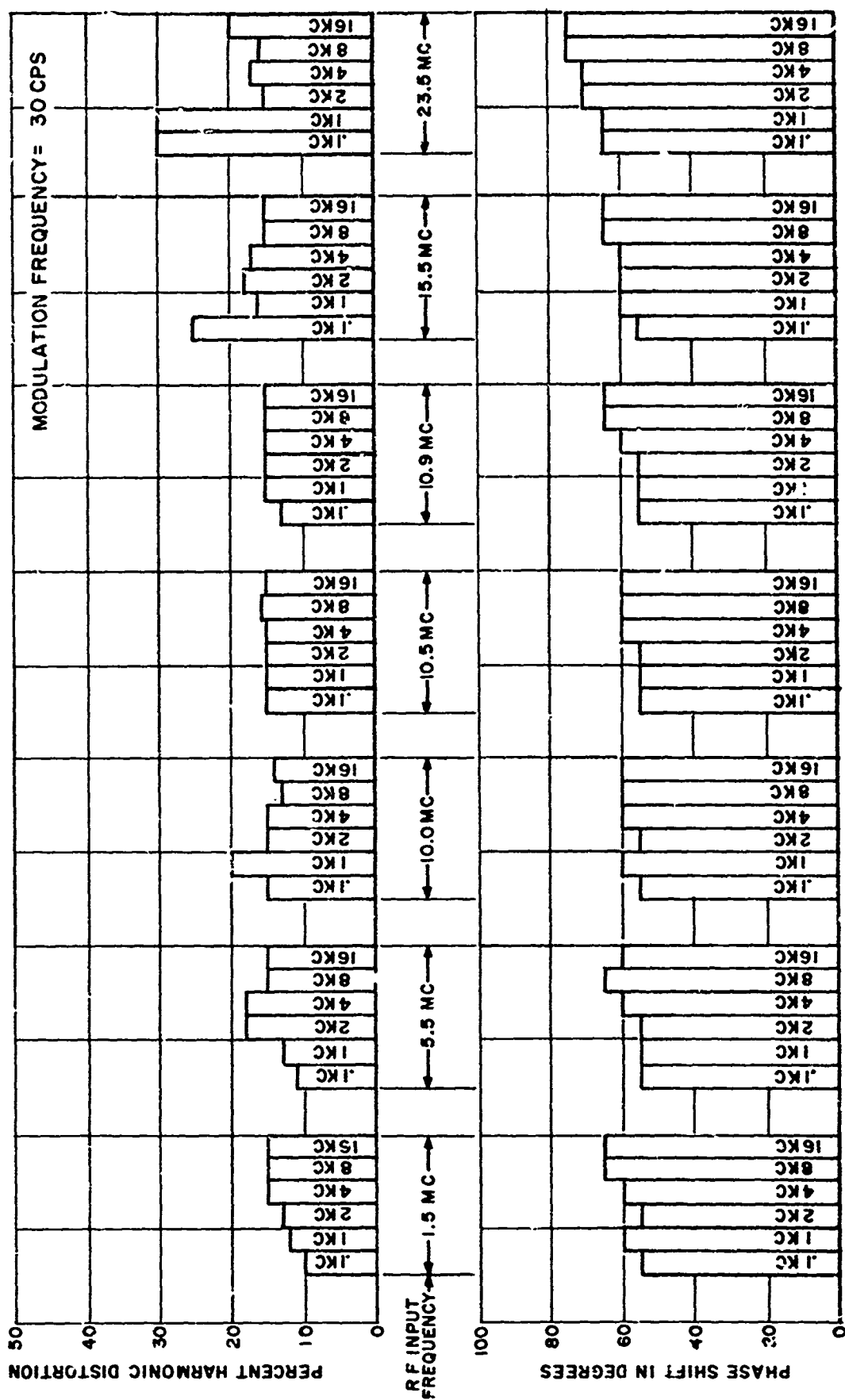
FIGURE 16.

R-390A PERCENT HARMONIC DISTORTION AND PHASE SHIFT FOR VARIOUS BANDWIDTHS.

34

cases the receiver was tuned for maximum IF output. Distortion and phase shift measurements were obtained for this tuning. It was found that virtually any value of phase shift could be obtained by tuning the frequency dial of the receiver. Hence, the absolute value of the phase shift measured here depends upon frequency tuning. It is seen that when a criterion of tuning is chosen, phase shift remains constant with a variation less than 10 degrees for any given frequency.

2.   RA. 17C Phase and Distortion Data

Corresponding data for the Racal RA. 17C receiver were obtained to determine front-to-back phase shift and distortion as a function of bandwidth. The frequencies at which phase measurement was obtained were 1.5, 5.5, 10, 10.5, 10.9, 15.5 and 23.5 mc. Distortion measurements were made at 1.5, 5.5, 10, 5, 15.5 and 23.5 mc. These data are shown in Figure 17. In all cases, the receiver was tuned for a maximum IF output. Phase shift and percent harmonic distortion were then determined. It is seen from the data of Figure 17 that phase shift measurements could be made for the 1.2-kc, 3-kc, 6.5-kc and 13-kc bandwidths at all frequencies. At 1.5 mc the 0.1- and 0.3-kc bandwidths could be measured in addition to other bandwidths. The 1.2- to 13-kc bandwidths show a maximum variation of phase shift as great as 15 degrees at the 10 mc frequencies. Fifteen degrees phase shift as a function of bandwidth was also observed at 15.5 mc. At 1.5 mc a 65-degree change of phase shift as a function of bandwidth was obtained where phase shift was measured at all bandwidths from 0.1 kc to 13 kc.

The percent harmonic distortion data show distortion approaching 50 percent for the 0.1- and 0.3-kc bandwidths at frequencies of 10.5 mc and 15.5 mc. Harmonic distortion was so severe at the lowest bandwidths that phase shift data could be obtained only at the lowest frequency. At no time did the phase shift change as a function of time for a given bandwidth setting. However, it was found that virtually any phase shift desired could be tuned as a function of tuning frequency. After a tuning criterion is established, phase shift as a function of bandwidth remains constant within 15 degrees for all frequencies for the bandwidths greater than 0.3 kc.

The phase shift data presented for the R-390A and RA. 17C show significant harmonic distortion for all bandwidths, i.e., harmonic distortion exceeding 10 percent in all cases. Although apparently this distortion can be tolerated at the widest bandwidths for D/F applications, as seen in the preceding section, excessive harmonic distortion results in bearing error which is intolerable for D/F applications. In particular, the wide variation of phase shift as a function of tuning frequency results in phase shift of the sidebands and hence bearing error which was observed and reported in section A. 3. (d).
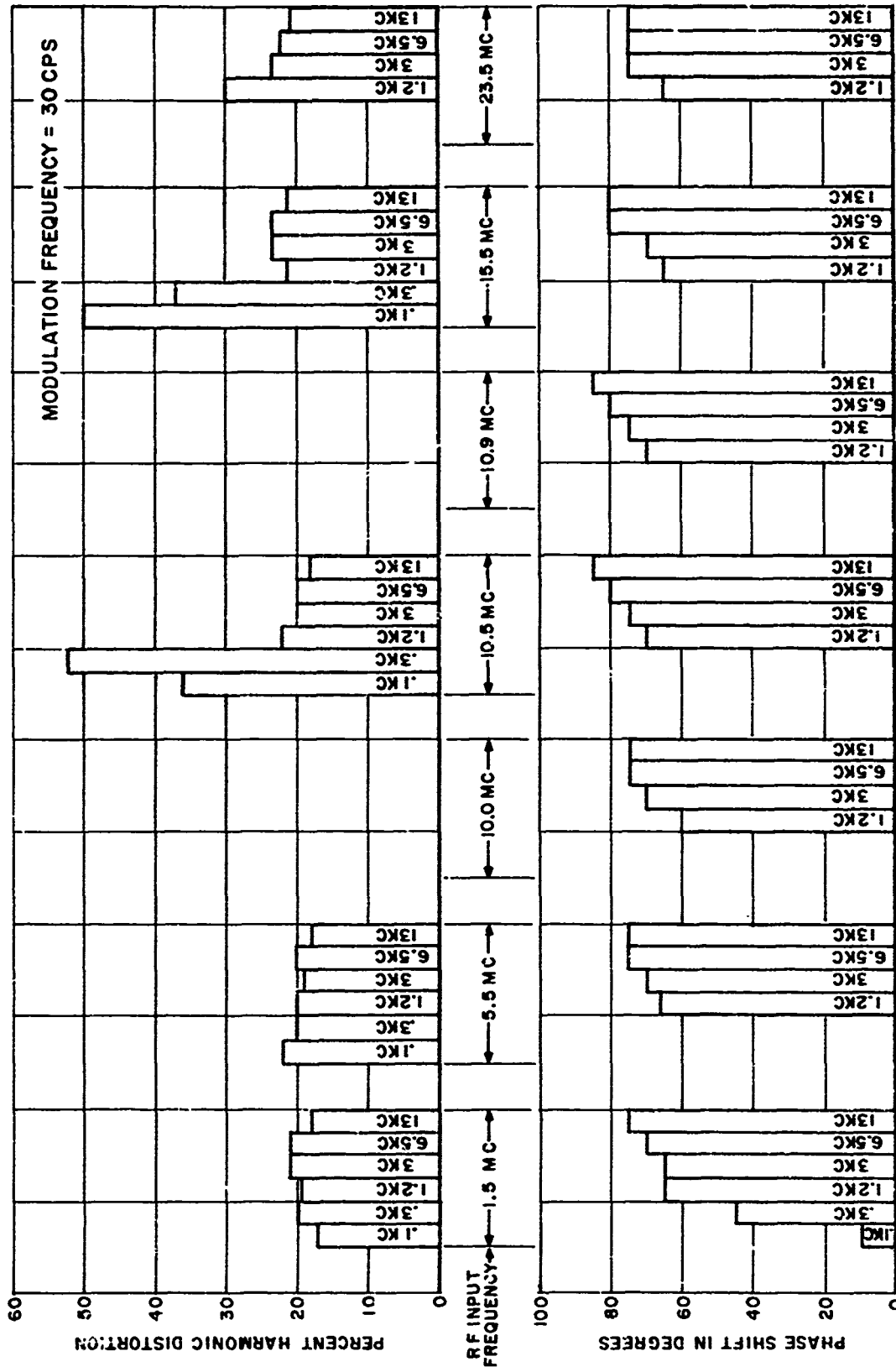
FIGURE 17.

RA.17C PERCENT HARMONIC DISTORTION AND PHASE SHIFT FOR VARIOUS BANDWIDTHS.

C.   Polarization Response of Spaced Loop Antennas

During the past interim, an investigation of multipolarization
D/F antennas was begun.   The polarization response of the spaced loop
and 8-loop antennas has been derived and is presented below.

The geometric configuration of two loops separated in space is
utilized with appropriate interconnection to produce the four-null antenna
pattern used for D/F purposes.   Three configurations of the spaced loops
of interest to direction finding are shown in Figure 18, namely the coaxial,
vertical coplanar, and horizontal coplanar spaced loops.   These antennas
may be rotated or combined in 4-loop arrays of two perpendicularly
crossed pairs as shown in Figure 18b to produce the D/F characteristics
desired.   Each of these spaced loop configurations will be analyzed as
regards their response to vertical and horizontal polarization in the
following paragraphs.   A summary of the polarization response of each
pair is given at the end of this section in Figure 20.

1.   The Spaced Loop as a Linear Array

Although multiloop arrays have been treated in a number of
ways, treatment of the spaced loop as a two-element linear array is
adopted here for brevity in deriving its basic D/F properties.   The sketch
of Figure 19 shows the geometric arrangement of the spaced loops as a
linear array.

The array factor for the spaced loop configuration is the
same for all configurations of spaced loops.   This array factor is derived
in the following manner.   Consider harmonically varying plane waves
incident upon the origin of the array coordinate system as shown in Figure
19a.   The array configuration is that of two isotropic radiators separated
by a distance d/2 on each side of the origin.   The two patterns may be
either added or subtracted algebraically as.

Array pattern algebraic difference

$$A_d = e^{j\frac{\beta d}{2}\cos\phi} - e^{-j\frac{\beta d}{2}\cos\phi}$$

$$= 2j\sin\left[\frac{\beta d}{2}\cos\phi\right]$$

Array pattern algebraic sum

$$A_s = e^{j\frac{\beta d}{2}\cos\phi} + e^{-j\frac{\beta d}{2}\cos\phi}$$

$$= 2\cos\left[\frac{\beta d}{2}\cos\phi\right]$$
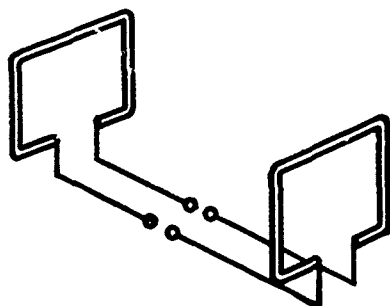
a.SPACED LOOP PAIR b.FOUR LOOP ARRAY
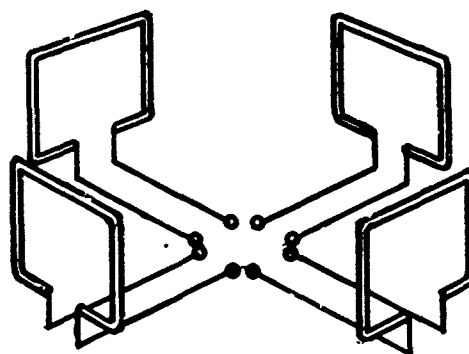
COAXIAL SPACED LOOPS

VERTICAL COPLANAR SPACED LOOPS

HORIZONTAL COPLANAR SPACED LOOPS

FIGURE 18.

SCHEMATIC PRESENTATION OF SPACED LOOP ANTENNAS.

a. ARRAY GEOMETRY

COAXIAL SPACED LOOP

VERTICAL COPLANAR
SPACED LOOP

HORIZONTAL COPLANAR
SPACED LOOP
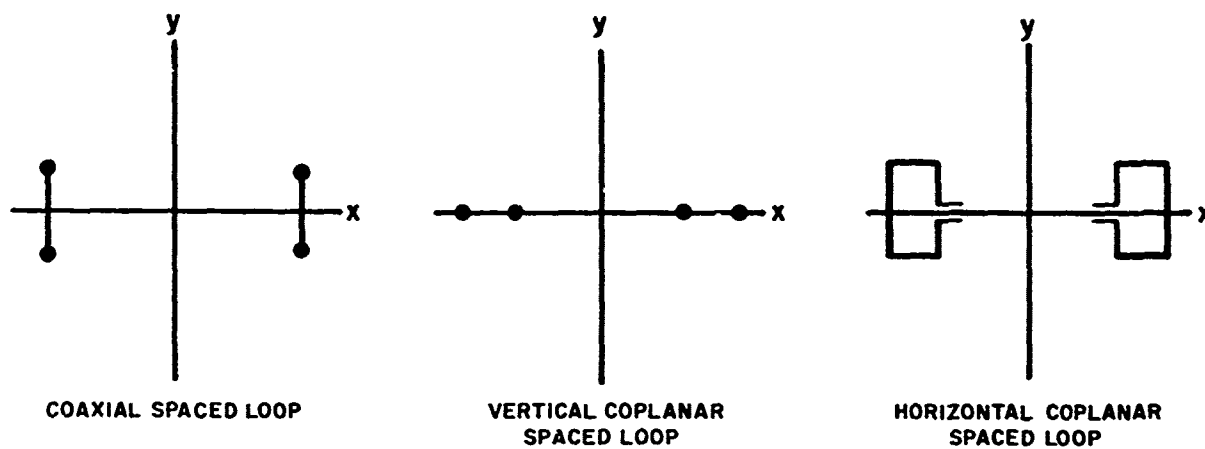
b. ELEMENT GEOMETRY

FIGURE 19.

THE SPACED LOOP ANTENNA AS A LINEAR ARRAY.

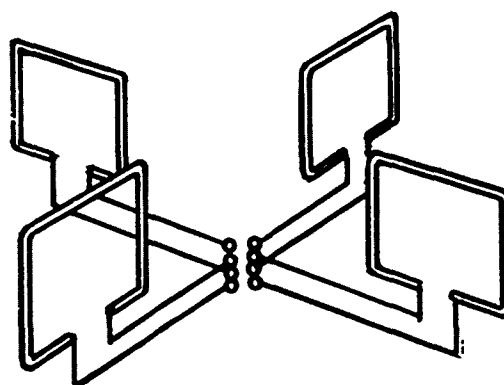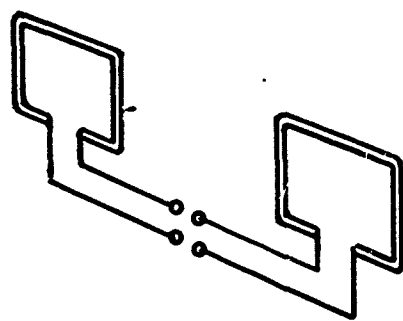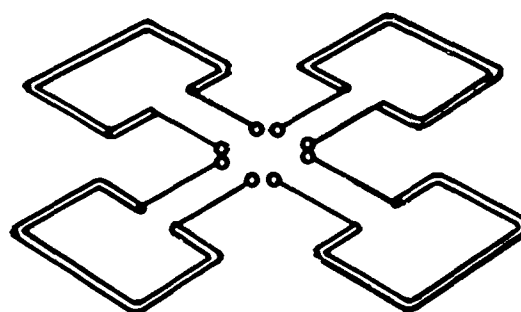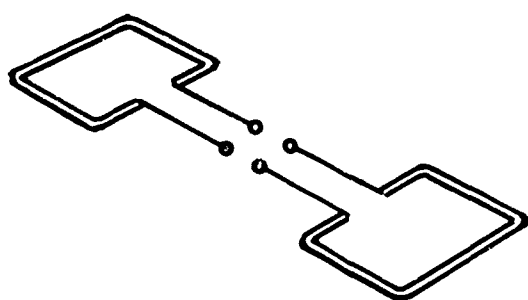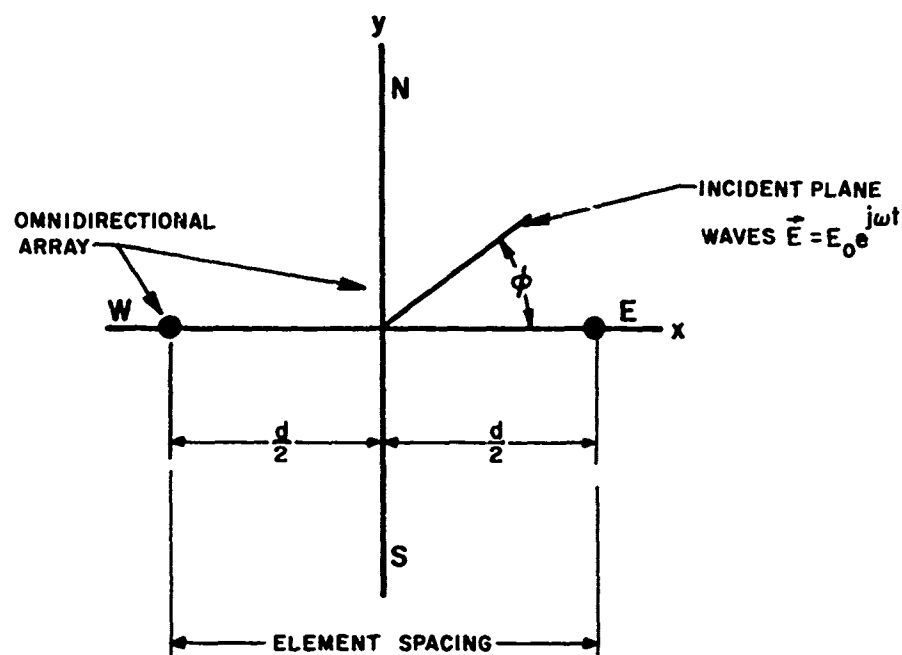| CONFIGURATION OF SPACED LOOP PAIRS	LOOP CONNECTION		POLARIZATION	
	ALGEBRAIC SUM (EW+NS)	ALGEBRAIC DIFFERENCE (EW−NS)	VERTICAL	HORIZONTAL
COAXIAL SPACED LOOPS	················	E-W SPACED LOOP	$-\beta^2\sin 2\phi$	$-\beta^2\cos^2\phi$
	················	N-S SPACED LOOP	$+\beta^2\sin 2\phi$	$-\beta^2\sin^2\phi$
	4 LOOP ARRAY	················	$-\beta^4\sin 4\phi$	$-\beta^2(1)$
	················	4 LOOP ARRAY	$-2\beta^2\sin 2\phi$	$-\beta^2\cos 2\phi$
VERTICAL COPLANAR SPACED LOOPS	················	E-W SPACED LOOP	$-\beta^2\cos^2\phi$	$-\beta^2\sin 2\phi$
	················	N-S SPACED LOOP	$-\beta^2\sin^2\phi$	$+\beta^2\sin 2\phi$
	4 LOOP ARRAY	················	$-\beta^2(1)$	$-\beta^4\sin 4\phi$
	················	4 LOOP ARRAY	$-\beta^2\cos 2\phi$	$-2\beta^2\sin 2\phi$
HORIZONTAL COPLANAR SPACED LOOPS	················	E-W SPACED LOOP	O	$-\beta^2\cos\phi$
	················	N-S SPACED LOOP	O	$-\beta^2\sin\phi$
	4 LOOP ARRAY	················	O	$-\beta^2(\cos\phi+\sin\phi)$
	················	4 LOOP ARRAY	O	$-\beta^2(\cos\phi-\sin\phi)$

NOTE: THE POSITIVE SIGN (+) IN THE ABOVE ANTENNA PATTERN EQUATIONS DENOTES SIGNAL IN PHASE WITH AN OMNIDIRECTIONAL ANTENNA. THE NEGATIVE SIGN (−) DENOTES 180° OUT OF PHASE WITH AN OMNIDIRECTIONAL ANTENNA.

FIGURE 20.

TABLE OF AZIMUTH PLANE ANTENNA PATTERNS FOR SPACED LOOP ANTENNAS.

where

$$\beta = \frac{2\pi}{\lambda} \, , \quad \text{the free space phase constant}$$

d = array element spacing

ϕ = azimuth angle

Now for cases of practical significance $\lambda >> d$, thus the array factors become

$$A_d \cong j \beta d \cos \phi$$

$$A_s \cong 2$$

The element patterns and the polarization response of the spaced loop array will be considered in turn in the paragraphs to follow.

2.   Coaxial Spaced Loop

a.   Vertical Polarization

The diagram of Figure 19b shows a view of the X-Y plane in which the vertical elements of the loop appear as points. The voltage signal induced on each of the vertical conductors of the loop is given by

$$\left| \int \vec{E} \cdot \vec{d\ell} \right| = \left| E_o \ell \, e^{j\omega t} \right|$$

where E_o = the amplitude of the incident waves, and ℓ = the conductor length. The phase relation between the loop conductors is given by

$$\left(e^{j\beta r \sin \phi} - e^{-j\beta r \sin \phi} \right) = 2j \sin(\beta r \sin \phi)$$

thus, the element pattern (P_E) is given by

$$P_E = 2j E_o \ell \, e^{j\omega t} \sin(\beta r \sin \phi)$$

and for $r << \lambda$

$$P_E \cong 2j E_o \ell \, e^{j\omega t} \beta r \sin \phi$$

The (sin 2ϕ) antenna pattern for the coaxial spaced loop for vertical polarization (V_T) is therefore given by

$$V_T^V = A_d P_E$$

$$= -E_o V \beta^2 \sin 2\phi$$

where $V = rd\ell$, the effective spaced loop volume.

If the loop is rotated at a speed Ω degrees per second, V_T^V becomes

$$V_T^V = -E_o V \beta^2 \sin 2(\phi - \Omega)$$

The nulls are displayed and bearings are taken by the usual single channel automatic bearing indicator method.

In order to obtain mutual coupling symmetry between elements of the nonrotating spaced loop, another pair of loops is added along the y axis. Hence, the apparent bearing of the incident wave to this pair is given by

$$V_T^{'V} = -E_o V \beta^2 \sin 2\left(\phi + \frac{3\pi}{2}\right)$$

$$= + E_o V \beta^2 \sin 2\phi$$

Thus, in order to obtain the sin 2ϕ spaced loop pattern, the two perpendicular spaced loop pairs must be algebraically subtracted at the crossover point to yield

$$V_{4\text{-loop}}^V = V_T^V - V_T^{IV}$$

$$= -2 E_o V \beta^2 \sin 2\phi$$

b.   Horizontal Polarization

For the case of horizontal polarization, the coaxial spaced loop amplitude function is given by

$$\left| \int \vec{E} \cdot \vec{d\ell} \right| = \left| E_o \ell \cos \phi \right|$$

The phase portion of the response is given by

$$\left(e^{j\beta r \cos \theta} - e^{-j\beta r \cos \theta} \right) = 2j \sin (\beta r \cos \theta)$$

where θ is the polar angle with respect to the z axis. For cases of practical significance $\lambda \gg r$, therefore, the horizontal response is given by

$$V_T^H = A_d \cdot P_E$$

$$V_T^H = -2 E_o \ell \cos \phi \cdot 2j\beta r \cos \theta \cdot j\beta d \cos \phi$$

$$= -2 E_o V \cos \theta \cos^2 \phi$$

For the spinning coaxial spaced loop for horizontal polarization, it is seen that the two nulls in the $\phi = \delta$, $\delta + \pi$ direction remain constant irrespective of polarization. However, the 4-loop response is given by the algebraic difference of the two spaced loop pairs

$$V_{4\text{-loop}}^H = V_T^H - V_T'^H = - V E_o \cos \theta \beta^2 (\cos^2 \phi - \sin^2 \phi)$$

$$= E_o V \beta^2 \cos \theta \cos 2\phi$$

and hence produces a 90-degree bearing shift for horizontal with respect to vertical polarization. Such performance is similar to the simple loop and hence the antenna is not suitable for D/F applications involving both horizontal and vertical polarization.

It is noted that for the algebraic sum connection the 4-loop antenna produces a sin 4ϕ pattern. However, practical attainment of this pattern is extremely difficult due to the severe reduction of the effective height (h_e) which possesses a β^4 term.

3. The Vertical Coplanar Spaced Loop

a. Vertical Polarization

The element pattern for the vertical coplanar spaced loop is given by

$$P_E^V = E_o \ell \, e^{j\omega t} 2j \sin (\beta r \cos \phi)$$

which for $\lambda \gg r$ is

$$P_E^V = 2j E_o \ell \, e^{j\omega t} \beta r \cos \phi$$

Thus, the spaced loop equation given by multiplication of the array factor with the element factor is

$$v_T^V = P_E \cdot A_d$$

$$= - V E_o \beta^2 \cos^2 \phi$$

The spinning spaced loop equation becomes

$$v_T^V = - V E_o \beta^2 \cos^2 (\phi - \Omega)$$

For the case of the 4-loop vertical coplanar spaced loop, a four-null pattern results for the case of algebraic subtraction of the two perpendicular spaced loop responses as above for the coaxial case. The response equation is

$$v_{4\text{-loop}}^V = - E_o V \beta^2 \cos 2\phi$$

b.   Horizontal Polarization

By argument analogous to that given for the coaxial spaced loop, the horizontal response pattern for one loop pair is

$$P_E^H = E_o \ell\ e^{j\omega t} \sin \phi\ (e^{j\beta r \cos \theta} - e^{-j\beta r \cos \theta})$$

The total response thus becomes for algebraic subtraction

$$V_{4\ \text{loop}} = - E_o V \beta^2 \cos \theta \sin 2\phi$$

It is seen that a 90°-bearing shift is obtained for horizontal polarization with respect to vertical polarization for the vertical coplanar spaced loop. This characteristic makes this antenna unsuited for testing bearings on signals of mixed polarization.

4.   The Horizontal Coplanar Spaced Loop

a.   Vertical Polarization

From Figure 19b, it is seen that the horizontal spaced loop has all its conductors cross-polarized to vertical polarization. Thus, in all its connection modes, the horizontal coplanar spaced loop is insensitive to vertical polarization. The radiation pattern for vertical polarization is zero.

b.   Horizontal Polarization

The response of the loop elements to horizontal polarization is given by

$$P_E^H = E_o \ell \, e^{j\omega t} [\cos \phi \, (e^{j\beta r \cos \phi} - e^{-j\beta r \cos \phi})$$

$$+ \sin \phi \, (e^{j\beta r \sin \phi} - e^{-j\beta r \sin \phi})]$$

The first term is due to the horizontal conductors parallel to the y axis in Figure 19b, and the second term is due to the horizontal conductors parallel to the x axis. Thus, the element pattern for $\lambda \gg r$ is given by

$$P_E^H = +j2\beta\ell \, r(\cos^2 \phi + \sin^2 \phi) = 2j\beta r\ell$$

The horizontal coplanar space loop pattern is therefore given by

$$V_{4\text{-loop}}^H = -\beta d \cos \phi \, \ell \, \beta r$$

$$= -2\beta^2 r^2 d \cos \phi$$

where $\ell = 2r$. Thus, it is seen that the horizontal coplanar spaced loop possesses simple loop response with reduced effective height because of the β^2 factor where $\beta \ll 1$. Thus, the horizontal coplanar spaced loop possesses none of the advantages of either the coaxial or vertical coplanar spaced loop configurations.

D.   Other Project Work

1.   Hybrid Transformer

A hybrid transformer for use with a spaced loop pair will yield both the simple loop signal and the spaced loop signal from the same pair of loops. This simple loop signal can then be used to sense the spaced loop D/F indication in either the twin channel system or the goniometer scan system. The development of a suitable hybrid transformer was continued on a limited basis during the past interim period.

New models of the hybrid transformer have been designed utilizing transmission line transformers constructed by forming the transmission line with a winding on small toroidal ferrite cores as described by Ruthroff.[16] Hybrid transformers constructed by this technique have low insertion losses. However, because three different types of windings

---

[16]Ruthroff, C. L., "Some Broad-Band Transformers," Proceedings of the IRE, Vol. 47, Nr. 8, August 1958, pp. 1337-1342.

on individual cores are required for a hybrid transformer with two balanced inputs suitable for loop antennas, it is difficult to avoid phase shift differ- ences as a function of frequency in the difference output mode of the trans- former which produce distortion in the spaced loop pattern. The crossover connection of a coaxial spaced loop is extremely critical requiring all leads to the individual loops to have exactly the same electrical length. The sum mode yields good simple loop patterns.

A field pattern obtained from the difference mode with a hybrid transformer of current design at 10 mc is given in Figure 21. The spaced loop pattern obtained when the loops of the system were connected in a normal crossover connection without the hybrid transformer is given for comparison. The dipole distortion in the hybrid pattern indicates objectionable phase shift in the transformer comparable to an unbalanced crossover network. Patterns obtained with the hybrid transformer above and below 10 mc had increased distortion.

2. The DFG-4 UHF Direction Finder

The Servo Corporation DFG-4 Doppler UHF direction finder equipment has been prepared for shipment. Necessary mechanical informa- tion on the DFG-4 antenna has been obtained and placed on file for the design of flexible mounting hardware to enable the antenna to be mounted in several unfavorable positions on a ship for bearing error tests. Travel to Newport, Rhode Island, is anticipated early in the next interim period to select suitable sites on a designated ship and to obtain the necessary information to complete the design of the mounting hardware.
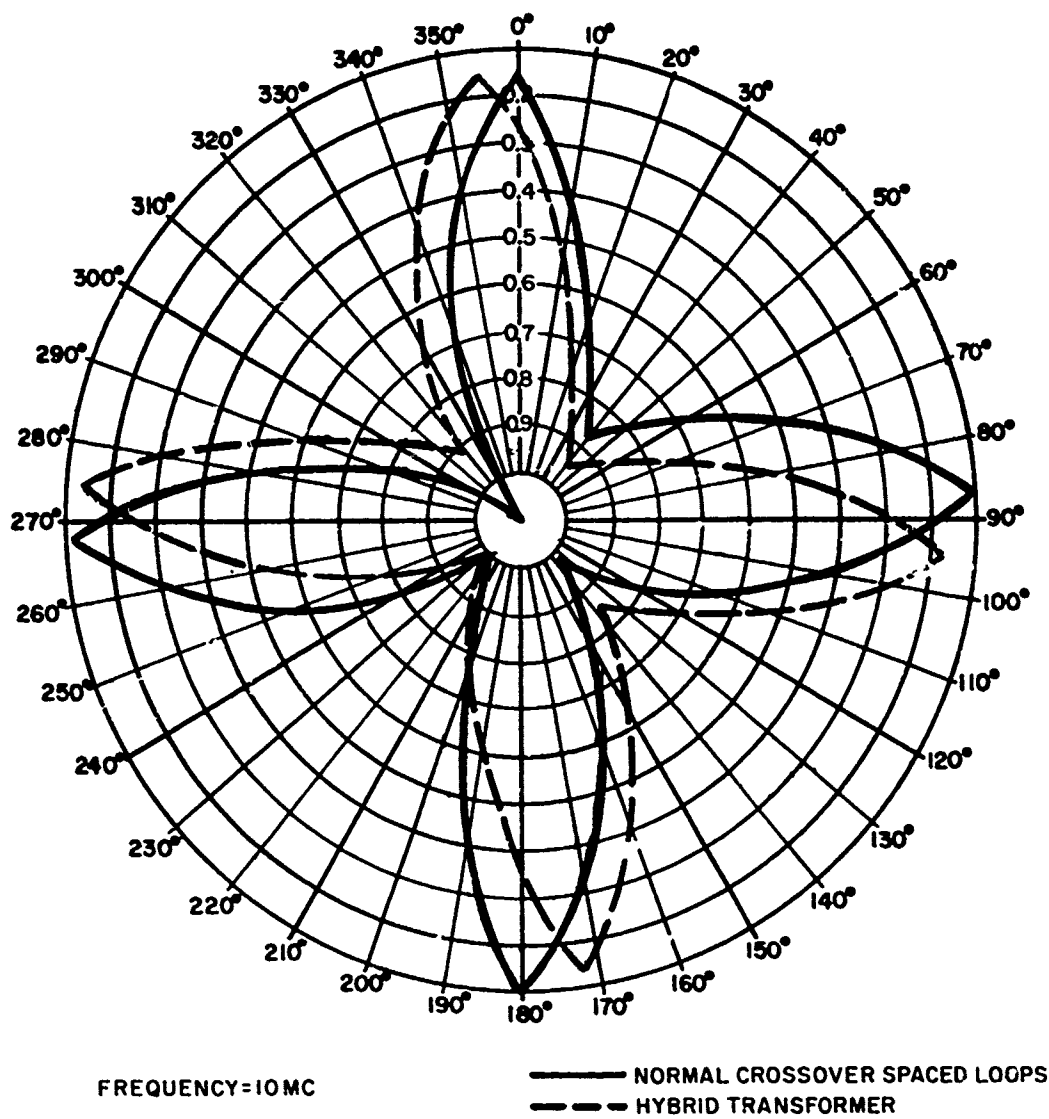
FREQUENCY=10MC

━━━━━ NORMAL CROSSOVER SPACED LOOPS
━ ━ ━ HYBRID TRANSFORMER

FIGURE 21.

SPACED LOOP PERFORMANCE WITH A HYBRID TRANSFORMER.

CONCLUSIONS

1.   The 8-loop spaced loop antenna may be operated through the self-resonant frequency without excessive bearing error, provided the antennas are resonated to the same frequency and shunted by some resistance. No significant sensitivity sacrifice is introduced by these changes.

2.   The bearing error performance of a goniometer scan technique and the twin channel technique with the 17-foot diameter 8-loop antenna is approximately equivalent.

3.   The standard model R-390A and RA.17C communications receivers, when used as D/F receivers, were found to introduce bearing shift greater than ± 1° for IF bandwidths less than 6.5 kc.

4.   Phase shift (envelope phase delay) through the R-390A and RA.17C receivers was observed to be constant within 15° as a function of bandwidth for both receivers. However, excessive harmonic distortion of AM signals was observed for bandwidths less than 1.2 kc.

5.   Theoretical investigation of the polarization response of various spaced loop antennas has shown that the fixed arrays studied for use with the twin channel or goniometer technique were not suitable for taking bearings on both vertically and horizontally polarized signals. The 8-loop antenna under investigation, however, does possess reradiation error advantages for shipboard use for vertical polarization.

6.   The hybrid transformer is a suitable technique for obtaining the spaced loop and simple loop signals from the same loop pair. However, an extensive research and development effort will be necessary to produce an aperiodic hybrid transformer for the 2- to 160-mc frequency range.

PROGRAM FOR NEXT INTERVAL

1.   Continue development of the twin channel 8-loop D/F system.

2.   Continue development of the 8-loop goniometer D/F system parallel to the twin channel development.

3.   Initiate tests of the 8-loop antenna and derivations therefrom in a through-mast configuration (antenna concentric with the mast).

4.   Investigate tuning of the individual spaced loops of the 8-loop antenna to increase sensitivity or to reduce physical dimensions of the antenna.

5.   Continue investigation of new antennas for shipboard D/F systems with emphasis on antennas with advantages over the simple loop for reradiation error and polarization response.

6.   Conduct tests of the Servo DFG-4 Doppler equipment on a ship to be designated.

7.   Begin development of goniometers for the 30- to 160-mc frequency range.

8.   Initiate planning for shipboard tests of the 3-loop antenna in an available site for comparison with results obtained for the optimum site on the U.S.S. Kraus.

IDENTIFICATION OF PERSONNEL

Personnel assignments to the project along with their man-hour contributions for the period from 16 April 1962 to 4 August 1962 are shown listed below. These are nominal assignments and are subject to change in future reporting periods as project assignments vary.

W. Lyle Donaldson, Director	104.0
Dr. W. J. McGonnagle, Assistant Director	88.0
Douglas N. Travers, Manager, Radio Direction Finding Research	512.0
Herman F. Barsun, Senior Research Engineer	6.0
Ray E. Cooper, Senior Research Engineer	80.0
Wray Fogwell, Senior Research Engineer	88.0
C. J. Laenger, Senior Research Engineer	40.0
John D. Moore, Senior Research Engineer	580.0
William E. Oakey, Senior Research Engineer	112.0
Paul E. Martin, Research Engineer	300.0
W. M. Sherrill, Research Engineer	612 0
H. C. Shouse, Electromechanical Designer	30.0
H. Stanley Benson, Senior Electronic Technician	171.0
Phil R. Clark, Senior Electronic Technician	571.0
J. W. Cuccia, Senior Electronic Technician	64.0
Stuart M. Hixon, Senior Electronic Technician	32.0
Tom E. Moorman, Senior Electronic Technician	462.0
F. W. Schrader, Senior Electronic Technician	8.0
John Arambula, Electronic Technician	40.0
Dan Gillespie, Electronic Technician	208.0
Joe Rodriquez, Electronic Technician	52.0
R. L. Seward, Electronic Technician	268.0
Bill Stevens, Electronic Technician	12.0
Herbert E. Kohler, Senior Draftsman	171.0
J. B. Perera, Draftsman	145.0
M. Pike Castles, Student Engineer	112.0
W. Braymen, Laboratory Assistant	8.0
Jack Lively, Laboratory Assistant	40.0
Walter Pish, Laboratory Assistant	16.0
Gordon K. Price, Laboratory Assistant	73.0
Don M. Stone, Laboratory Assistant	224.0
Direct Project Assignment (Total of Above)	5229.0
Other Southwest Research Institute Personnel	190.6
Total Man-Hours for all Charges	5419.6